EM Photonics

October 12, 2006

Air Force FY2004 Phase II SBIR/STTR

Technical Topic Number: AF02T017, Nanophotonics

Contract Title: Photonic Band Gap Devices for Commercial Applications

Contract Number: FA9550-04-C-0062

Contractor: EM Photonics, Inc.
51 E. Main Street Suite 203
Newark, DE 19711
Phone (302) 456-9003
FAX (302) 456-9004

Principal Investigator: Dr Ahmed Sharkawy

Additional EM Photonics Investigators: Dr. Shouyuan Shi
Dr. Caihua Chen

STTR Partner: Dr. Dennis Prather (PI)
University of Delaware
Electrical and Computer Engineering Department
Evans Hall
Newark, DE 19716

Dates Covered: Jan, 2006- July 14, 2006

Photonic Bandgap Devices for Commercial Applications

REPORT DOCUMENTATION PAGE	Form Approved OMB No. 074-0188

Public reporting burden for this collection of information is estimated to average 1 hour per response, including the time for reviewing instructions, searching existing data sources, gathering and maintaining the data needed, and completing and reviewing this collection of information. Send comments regarding this burden estimate or any other aspect of this collection of information, including suggestions for reducing this burden to Washington Headquarters Services, Directorate for Information Operations and Reports, 1215 Jefferson Davis Highway, Suite 1204, Arlington, VA 22202-4302, and to the Office of Management and Budget, Paperwork Reduction Project (0704-0188), Washington, DC 20503

1. AGENCY USE ONLY (Leave blank)	2. REPORT DATE	3. REPORT TYPE AND DATES COVERED
	October/12/2006	Final Jan/01/2006 - July/14/2006

4. TITLE AND SUBTITLE
Photonic Bandgap Devices for Commercial Applications

5. FUNDING NUMBERS
FA9550-04-C-0062

6. AUTHOR(S)
Ahmed S. Sharkawy (PI)
Dennis W. Prather

7. PERFORMING ORGANIZATION NAME(S) AND ADDRESS(ES)

EM Photonics
51 East Main Street
Suite 203
Newark, DE 19711

8. PERFORMING ORGANIZATION REPORT NUMBER 03 (FINAL)

9. SPONSORING / MONITORING AGENCY NAME(S) AND ADDRESS(ES)

Air Force Office of Scientific Research
4015 Wilson Blvd Room 713
Arlington VA 22203-1954
Dr Gernot Pomrenke

10

AFRL-SR-AR-TR-06-0491

11. SUPPLEMENTARY NOTES
The views, opinions and/or findings contained in this report are those of the author(s) and should not be construed as an official Department of the Army position, policy or decision, unless so designated by other documentation.

12a. DISTRIBUTION / AVAILABILITY STATEMENT
Approved for public release: distribution unlimited.

12b. DISTRIBUTION CODE
UL

13. ABSTRACT ***(Maximum 200 Words)***

The overall objective of this STTR program is to *define and develop a unified manufacturing process for Photonic Band Gap (PBG) devices that combines design, simulation, fabrication, and test.* By investigating devices that serve the needs of current Air Force research programs, EM Photonics and the University of Delaware can achieve their technology transfer objectives and at the same time provide the most meaningful results to the Air Force. To achieve these goals we took a three tiered approach: (1) establish close working relationships with *two* AFRL research teams (one located at Hanscom, AFB, POC Dr. Richard Soref and the other at Write Patterson, AFB, POCs Drs. Anthony Crespo and Thomas Nelson); (2) identify and demonstrate the feasibility of suitable nano-photonic devices for rapid commercialization; and (3) explore further reaching and novel devices and fabrication processes for next generation photonic band gap technologies. Within the context of our Phase I effort we have succeeded in each of these areas and, as a result, are very anxious to begin a Phase II effort to continue our strong collaboration with the ARL researchers and the commercialization of nano-photonic devices.

14. SUBJECT TERMS
Photonic Crystals, Dispersion Properties, variable splitter, analog to digital converter, multi-spectral receiver

15. NUMBER OF PAGES
43

16. PRICE CODE

17. SECURITY CLASSIFICATION OF REPORT	18. SECURITY CLASSIFICATION OF THIS PAGE	19. SECURITY CLASSIFICATION OF ABSTRACT	20. LIMITATION OF ABSTRACT
UNCLASSIFIED	UNCLASSIFIED	UNCLASSIFIED	UL

TABLE OF CONTENTS

1 Abstract

In our effort to develop and demonstrate the design, fabrication, and experimental characterization of functional photonic crystal devices in both 2D and 3D structures, we identified various tasks and goals towards achieving the proposed applications. Two-dimensional photonic crystal structures will be used for in-plane optical signal distribution and routing while three-dimensional structures will be used for out-plane signal distribution, to provide high-density optically interconnected optoelectronic PhC circuits to distribute the optical signal between various circuits and in different angles.

Implementation of photonic crystal devices in planar dielectric slabs such as silicon-on-insulator (SOI) will not only open many exciting opportunities in integrated optics and high density optical interconnects but will also provide the basic building blocks for Nano-Photonic Circuits (NPC's). As the development of semiconductor, materials led to the current electronic revolution, photonic crystal device integration in planar dielectric slabs serves to hold the key to achieving the long-sought goal of large-scale integrated Photonic Circuits (LSPIC).

2 Problem Significance

Advances in integrated circuit manufacturing techniques have allowed for the miniaturization of devices on rapidly decreasing scales. In the last decade, we have witnessed the emergence of micro-electro-mechanical systems (MEMS) from the laboratory to a commercially viable industry reached $15 billion in sales in 2004.1 As MEMS technology has transferred to industry and the marketplace, research organizations have continued to pursue small-scale fabrication and have advanced to the submircon or nano regime. At these dimensions, where feature sizes are less than the wavelength of light, it is possible to produce optical materials and devices that allow for unique photonic control and manipulation. A new class of optical devices based on submicron periodic structures has emerged and is referred to as photonic crystals (PhC) or photonic band gap devices (PBGs). Preliminary research indicates that these devices will be capable of performing a wide variety of functions.2 These include but are not limited to switching, splitting, modulation, and filtering. PBGs can be integrated into small packages making them desirable for commercial applications such as optical interconnects and dense wavelength division multiplexing (DWDM), as well as military and government applications including quiet communications, sensors, and engineered coatings.

To fully realize the potential of PBG devices, there are several major research and development challenges that must be addressed. In fact, a recent report on the state of photonic integrated circuits suggests that the current obstacles to commercialization are software simulation, yields, materials, and test equipment. We agree and to this end, believe that we have assembled a team with the background and expertise to address these obstacles and bring this technology to market. EM Photonics, Inc. (EMP) is a Newark, Delaware small business that is developing devices and software products for micro and nano-photonics. The software products are based on the Finite-Difference-Time-Domain (FDTD) method and the Plane Wave Method (PWM) for electromagnetic. Both methods are implemented in 2 and 3 dimensional form. The software incorporates a user-friendly CAD interface that is compatible with many standard file formats and is capable of solving a wide variety of practical problems including PBG devices and systems. On the fabrication side, EMP is currently involved in projects for PBG devices, biosensors, military imaging systems, and commercial holography. At the University of Delaware, Dr. Prather's research program is internationally recognized for its work in

nanophotonics. The research program is unique in that it is equally strong in computational electromagnetics and nanofabrication. Dr. Prather receives funding from high visibility programs such as the AFOSR Nanophotonics program, DARPA's Advanced Lithography and OptoElectronic University Centers programs. His Nano-systems Technology Center maintains a sophisticated and specialized facility for the fabrication and characterization of nanophotonic devices. During the Phase I program, EMP and the University of Delaware demonstrated that the STTR is an ideal format for teaming. By investigating devices that serve the needs of current Air Force research programs, EMP and the University of Delaware were able to develop and demonstrate manufacturable processes based on Photonic Band Gap technology. The Phase I feasibility work served as a solid foundation for Phase II. In Phase II, processes was refined and resources dedicated to the production of functional devices for AFRL programs.

3 Project Overview

The overall objective of this STTR program is to *define and develop a unified manufacturing process for Photonic Band Gap (PBG) devices that combines design, simulation, fabrication, and test.* By investigating devices that serve the needs of current Air Force research programs, EM Photonics and the University of Delaware can achieve their technology transfer objectives and at the same time provide the most meaningful results to the Air Force.

To achieve these goals we took a three tiered approach: (1) establish close working relationships with *two* AFRL research teams (one located at Hanscom, AFB, POC Dr. Richard Soref and the other at Write Patterson, AFB, POCs Drs. Anthony Crespo and Thomas Nelson); (2) identify and demonstrate the feasibility of suitable nano-photonic devices for rapid commercialization; and (3) explore further reaching and novel devices and fabrication processes for next generation photonic band gap technologies. Within the context of our Phase I effort we have succeeded in each of these areas and, as a result, are very anxious to begin a Phase II effort to continue our strong collaboration with the ARL researchers and the commercialization of nano-photonic devices. Details of each aspect of our approach are presented in the remainder of this report.

U. S. Air Force Collaborations

A significant early accomplishment in our Phase II effort was the establishment of strong collaborative relationships with *two* Air Force research teams, which were centered on applications in Photonic Band Gap devices and systems. On November 17th , 2004, a kick-off meeting was held at the University of Delaware, in attendance were, Dr. Antonio Crespo, AFRL/SNDI, Dr. Dennis Prather, University of Delaware and Dr. Ahmed Sharkawy, EM Photonics, Inc. During the course of the meeting, Dr. Prather gave a presentation on his ongoing research programs at the University of Delaware and highlighted new facilities and equipments added to the current lab infrastructure. The University of Delaware purchased a new MBE system which will facilitate the growth of various materials. Such system will be highly beneficial to the current Phase II effort. Dr Sharkawy presented an overview of projects at EMP, in addition to stating the objectives of the STTR Phase II program.

4 Phase II Achievements

The original Phase I proposal outlined an ambitious array of tasks that were intended to flesh out the feasibility of nanophotonic photonic crystal based devices and explore the many new directions. We are pleased to report that all of the tasks we originally proposed have been completed successfully, with results that have surpassed our most optimistic expectations and convinced us of the enormous potential of functional photonic crystal and photonic bandgap devices. This section will review the tasks as proposed and summarize our progress.

In Phase I, we presented preliminary design and simulation for various device concepts in collaboration with AFRL researchers. In Phase II, we built on the success of Phase I results by carrying additional iteration stages where fabrication results were compared to initial design work. Additional designs were proposed, design and numerically simulated and finally fabricated. Finally the modeling and simulation tools developed as a results of this research were professionally packaged for commercial release and is currently available.

4.1 Part I: Photonic Crystal Based Analog to Digital Converter

Optical or optoelectronic analog-to-digital (A/D) converters have received significant interest due to the development of optical technologies in areas such as telecommunication, sensors, and imaging. Optical A/D converters may offer better performance than conventional electronic A/D converters, because optical signals are not subject to electronic noise and radiation, and are thus immunized from electromagnetic interference. Moreover, optical A/D converters eliminate the speed and sophistication limitation of electrical-to-optical and optical-to-electrical conversions in photonic networks. Several optical/optoelectronic A/D conversion approaches have been demonstrated, such as the Mach-Zender interferometer A/D converter [1, 2], the optical fiber temporal-spectral mapping A/D converter [3], the optoelectronic thyristor A/D converter [4], and the optical alternating layer A/D converter [5]. However, these designs are either optically or electrically sophisticated, or are not easy to be integrated. To this end, we propose an optical A/D converter based on planar photonic crystals (PhCs) [6]. As an example, a two-bit ADC is realized using three splitters in a self-guiding square lattice to achieve four distinct states. Each splitter is designed by simply changing the size of air holes along 45 degree to the propagation direction of the self-guiding beam to break the lattice uniformity and perturb the self-guiding beam. In addition, the self-guiding nature of the photonic crystal has the advantages of easy-coupling and zero-cross-talk signal crossing. Therefore, the resulting optical A/D converter is compact and easy to be integrated with other photonic components.

Dr. Antonio Crespo expressed interest in collaborating to design and implement a photonic crystal "analog to digital converter" (ADC), shown in Fig. 1. In this application, he proposed the use of a cascading array of beam splitters and detectors, to split the power of an incoming optical signal into multiple channels, by a specific percentage that correspond to a specific digital representation of the signal.

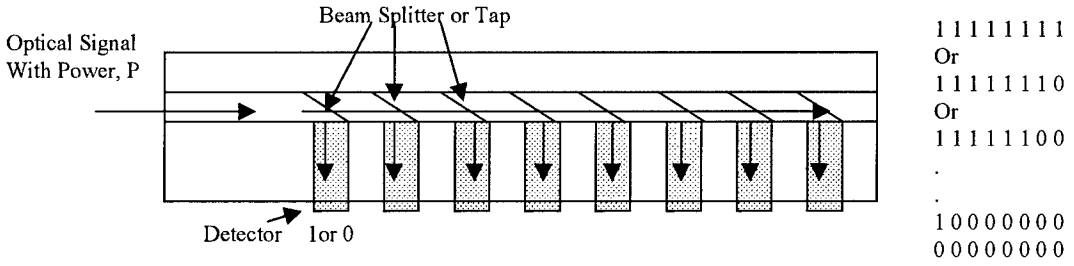

Figure 1: Analog to Digital Converter

Here, a strong signal will have enough energy for detection along the entire waveguide path. As the signal strength is reduced, the power progressively becomes too weak for detection at the most distant detectors. Thus, the digital representation follows the characteristics shown on the right of Figure 1 from the maximum to minimum power level.

Based on concept design provided by Dr Crespo, it was the role of EM Photonics researchers to determine the appropriate Photonic Crsystal based design which accounts for precise splitting ratios of the various beam splitters

A schematic of the proposed 2-bit A/D converter is shown in Fig. 2. In order to construct a 2-bit optical A/D converter, one needs four distinguishable states, which requires three splitters with splitting ratios of 50:50, 66:34, and 100: 0, respectively. These particular splitting ratios are chosen to consider the nonlinearity of the photodetector, which will be used to build the proposed A/D device. The concept of the 2-bit optical A/D converter is illustrated in Fig. 3. The input analog signal is assumed to be a sinusoidal wave. When the power of the incident wave is lower than twice the threshold value, namely $P_{in} < 2P_{th}$, the output powers at three output ports are smaller than the threshold level and the quantized states of three output ports is hence defined as '000'. When the input power is increased to $2P_{th}$, the output power at port I reaches threshold. Therefore, the states at the three output ports in this case can be similarly recognized as '100.' Accordingly, as the output power at ports II and III reach the threshold value, their states change from '0' to "1." Consequently, we have four different states, '000', '100', '110', and '111' at different levels of incident power. These four states can be coded into the desired four states "00", "01", "10", and "11" for a 2-bit optical A/D converter.

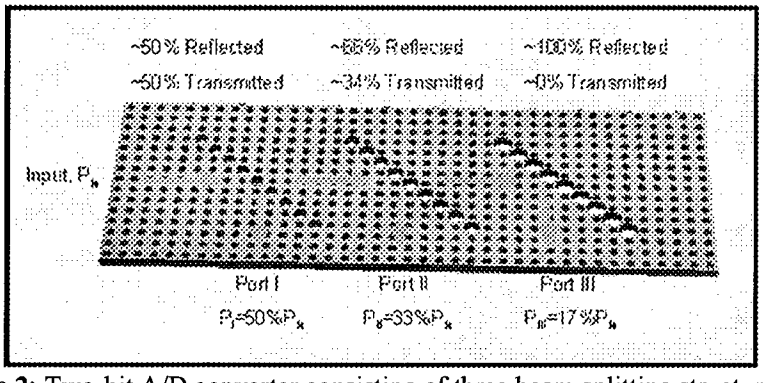

Figure 2: Two-bit A/D converter consisting of three beam splitting structures in a self-guiding photonic crystal

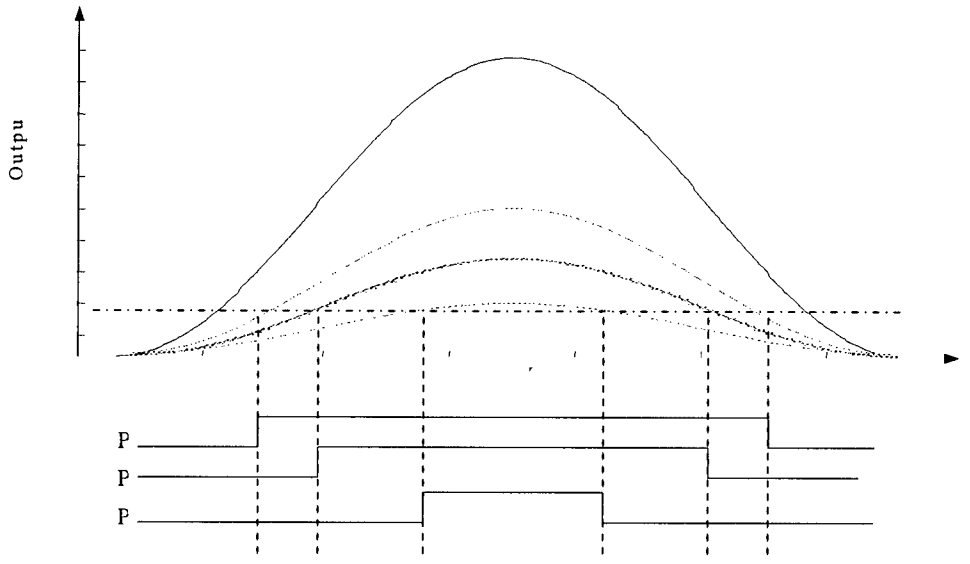

Figure 3: Concept of two-bit optical A/D converter..

4.1.1 Design 1: Low Resolution ADC using PhC Waveguides

After Air Force Researchers provided concepts and specifications, initial simulations were completed using EMPLab, a commercially available electromagnetic software package developed by EM Photonics.

Our initial ADC design was implemented using Photonic crystal waveguides with various tap angles to control the percentage of splitting required. Recall that in the ADC, by utilizing a cascading array of beam splitters and detectors, the power of an incoming optical signal can be represented digitally by considering the beam splitter percentage and the detector threshold. Based on this description, we have investigated beam-splitting methods that allow for a large range of splitting ratios with minimum back reflection. This is important because beam-splitting ratios may require precise adjustment for the correct digital representation. In addition, the waveguide configuration must be compact and easily integrated with a detector array.

Simulations were performed using EMPLab. Here, the PBG waveguide consisted of air holes in silicon, the lattice configuration was triangular, and the wavelength was ~1.6 microns. Beam splitting was accomplished by varying the angle of the splitting guide from 30 degrees to 60 degrees. At 30 degrees, a 90/10 splitting ratio was achieved. This is shown in Fig. 4.

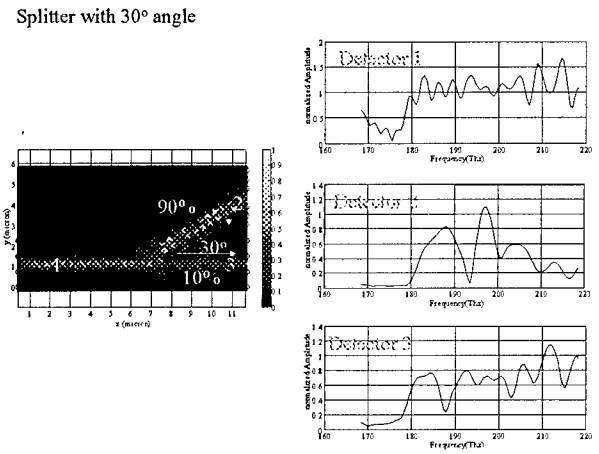

Figure 4: 90/10 Splitting Ratio

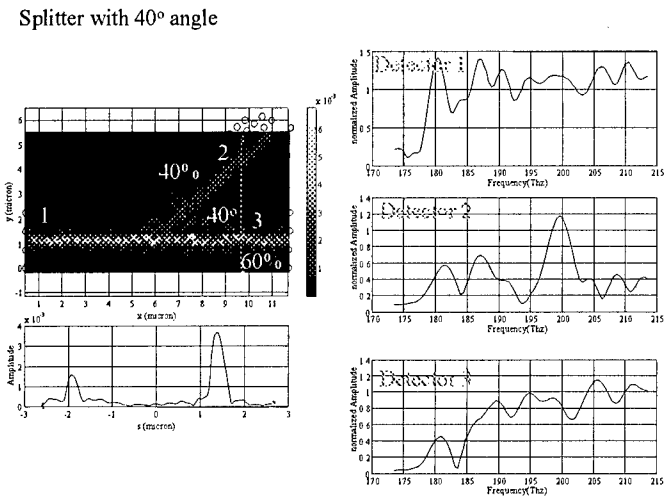

Figure 5: 40/60 Splitter

As shown in Figures 5 and 6, at 40 degrees, a 40/60 splitter was designed and at 45 degrees the splitting ratio was 25/75.

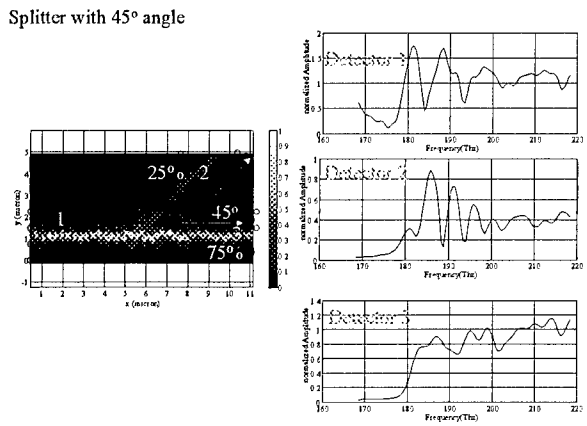

Figure 6: 25/75 Splitter

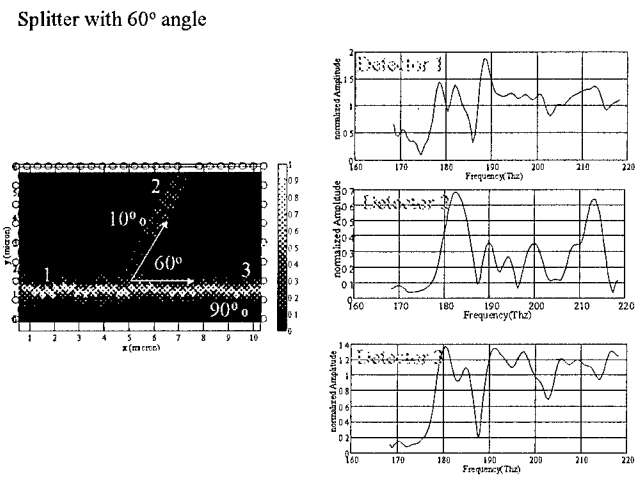

Figure 7: 10/90 Beam Splitter

Finally, at 60 degrees, a 10/90 splitting ratio was achieved. See Figure 7.

4.1.1.1 Fabrication of the Low Resolution ADC

Fabrication work was also accomplished on the ADC device proposed by Dr. Crespo. A 1-to-8 fan-out was fabricated using the 10%-90% splitters that were designed using EMPLab. Here, the lattice was triangular with a spacing of 450 nm and a cylinder size of 300 nm. Fig. 8 shows the full device, e-beam patterned in photoresist. The 8-splitter waveguides are oriented in a

horizontal direction. J-couplers are used to launch light into the primary guide and direct light out of the spitting guides.

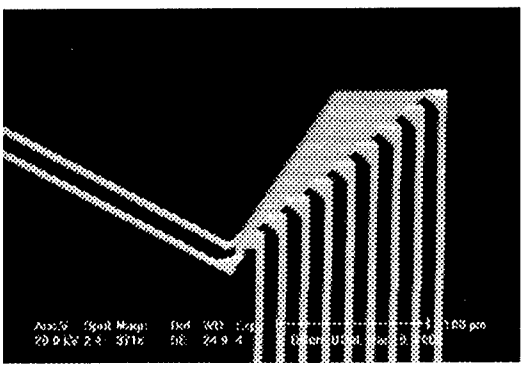

Figure 8: E-beam patterned J-Coupler

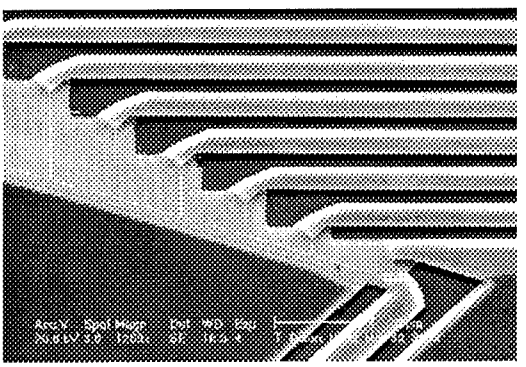

Figure 9: Optical Analog to Digital Converter, after etching.

Figure 9 shows the main waveguide and the first 5 splitter guides after etching. Here, the splitting waveguides are oriented in the vertical direction. Fig.10 shows a close up of the first splitter on the device.

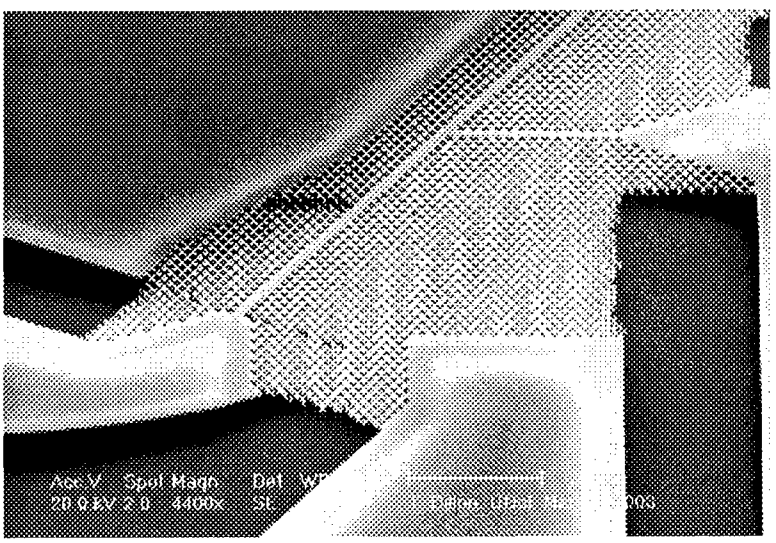

Figure 10: ADC, Main waveguide and first splitter

4.1.2 Design 2: High Resolution ADC using self-collimated PhC Waevgiudes

We examined another design for an ADC relying on engineering the dispersive properties of Photonic Crystals instead of their confinement properties. The design combines a self collimation photonic crystal structure with a mirror structure constructing the elements of the beam splitters.

By engineering the transmission/reflection properties of the mirrors structure high precision splitting ratios can be achieved and hence high-resolution ADC designs can be implemented

To design a 2-bit optical A/D converter, we first study a self-guiding lattice consisting of a square array of air holes patterned in a silicon slab. The lattice constant is 450 nm, the radii of air holes is 220 nm, and the thickness of the silicon slab is 240 nm, where a is the lattice constant. Figure 11 shows the dispersion properties of this lattice obtained using the iterative plane wave method [7], where (a) is the dispersion diagram and (b) is the dispersion equi-frequency contours (EFCs) [8] at frequencies (normalized to c/a, c is the light speed and a is the lattice constant) of 0.28, 0.285, 0.29, and 0.295. The solid grey area in (a) is the light cone, which indicates the radiation mode region (within the grey region) and well-confined mode region (outside the grey region) [9]. The plotted EFCs in (b) fall within the well-confined mode region. The represented modes can therefore be guided in the slab without any radiation loss. Moreover, as can be seen from (b) the EFC at the frequency of 0.295 is approximately flat along Γ-X direction except the round corners. Since the relation between the group velocity $\mathbf{v}_g$ and the dispersion function $\omega(\mathbf{k})$ can be expressed as:

$$\mathbf{v}_g = \nabla_k \omega(\mathbf{k}), \tag{1}$$

the group velocity, $\mathbf{v}_g$, or the direction of light propagation coincides with the direction of the steepest ascent of the dispersion surface, and is perpendicular to the EFC. Therefore, when one launches the incident beam with its wave-vector spectrum fallen in the approximately flat part of the EFC along the Γ-X direction, it is self-guided in the plane by the planar photonic crystal (PhC) [10]. To validate this, we launch a Gaussian beam into the lattice along the Γ-X direction and simulate the beam propagation within the lattice using the finite-difference time-domain (FDTD) method [11] with an effective index of 3.

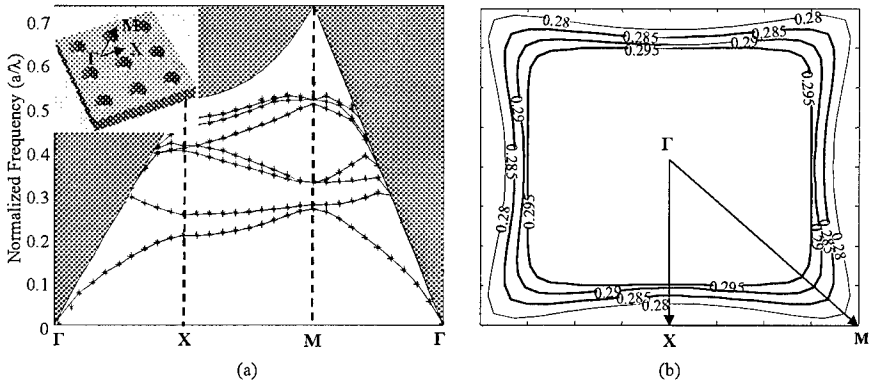

Figure 11: Dispersion properties of the square lattice patterned in a silicon slab with the radii of air holes of 0.25a and the slab thickness of 0.5333a: (a) dispersion diagram, (b) equi-frequency contours of the second band.

4.1.2.1 Design of a Single Splitting Unit

The optical beam splitter consists of two sections as shown in Fig. 12: a dispersion guiding PhC structure and a beam splitting structure. These PhC structures, with different radii, are both arranged on the same square lattice in a high index background of n=3.5. The PhC guiding structure has an air hole with a ratio $r_g = 0.3a$, where a is the lattice constant. The 45° rotated splitting structure has an air hole of radius r_s, which varies from $0.3a$ to $0.435a$. If the light is launched from port 0, then it will propagate through the dispersion guiding structure and arrive at the splitting structure. While passing through the splitting structure, the signal will be split between two orthogonal branches: one along the same direction as the incident wave, and exit at port 1, and the other portion along a direction orthogonal to the incident wave, and exit at port 2. The splitting percentage is proportional to the radius and number of layers of the splitting structure.

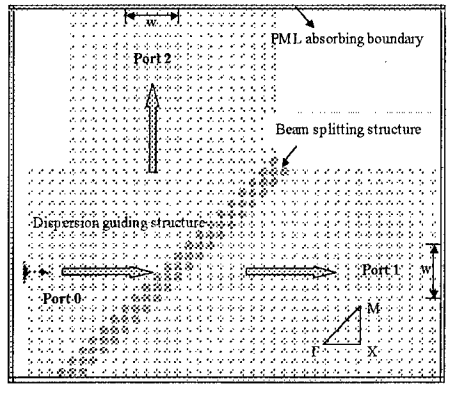

Figure 12: Dispersion based tunable beam splitter utilizing a hybrid PhC structure

Before we consider the beam-splitter structure, we first analyze the dispersion diagram of PhC structures. The dispersion properties of both types of photonic crystal structures can be obtained by using the plane wave method (PWM) [8]. The dispersion surfaces of PhCs can contain a variety of shapes depending on the lattice type, pitch, fill-factor, or index of refraction. By analyzing a cross-section of the dispersion surface at constant frequencies, one obtains equi-frequency contours (EFCs). The energy flow of light propagation, which is defined by the group velocity, $v_g = \nabla_k \omega(\mathbf{k})$, coincides with the direction of steepest ascent of the dispersion surface, thus perpendicular to the EFC. The EFCs of the second band for a square lattice photonic crystal with radius $r_g = 0.3a$ are shown in Fig. 2(a). It can be seen from the figure that the EFCs can be approximated by squares for normalized frequencies between 0.255c/a and 0.275c/a. For a square EFC, the wave is only allowed to propagate along directions normal to the sides of the square, $(\Gamma - X)$[5]. As shown in Fig. 2(a), one can vary the incident wavevector over $\pm 34^o$ and yet maintain a divergence angle less than $\pm 1^o$ at a normalized frequency of $0.26c/a$, .

It is interesting to note that as the radius of the air holes comprising the splitting structure increases, a stop band can be observed. The stop band must only be considered for incident angles in the range of $\pm 34^o$ to spatially match the acceptance cone of the self-guiding structure. The stop band map, which expresses the stop band variation as a function of the ratio r/a, is shown in Fig. 2(b). When the radius varies between 0.33a and 0.44a, a small stop band opens. However, because the stop band is very narrow, frequencies in the stop band and near the edge of the gap must be considered requiring more PhC layers to proportionally reflect incoming light. From Fig. 2(b), when the radii of air holes in the splitting region is between $0.374a$ and $0.437a$, the frequency $0.26c/a$ falls into the stop band and is primarily reflected by the splitting structure. Therefore, to obtain partial splitting, we vary the radius of the splitting structure air holes between $0.3a$ and $0.374a$. The equi-frequency contours for different radii of air holes are shown in Fig.2(c). Furthermore, as the radii of air holes increase, the EFC changes from a square to more concave shape. If the radii of air holes are between $0.3a$ and $0.34a$, the EFCs can still be

approximated as a square, enabling the optical wave to propagate through the splitter and exit at port 1, while the concave EFCs would cause the wave to diverge, employing only a few PhC layers for beam splitting ensures a small output beam width.

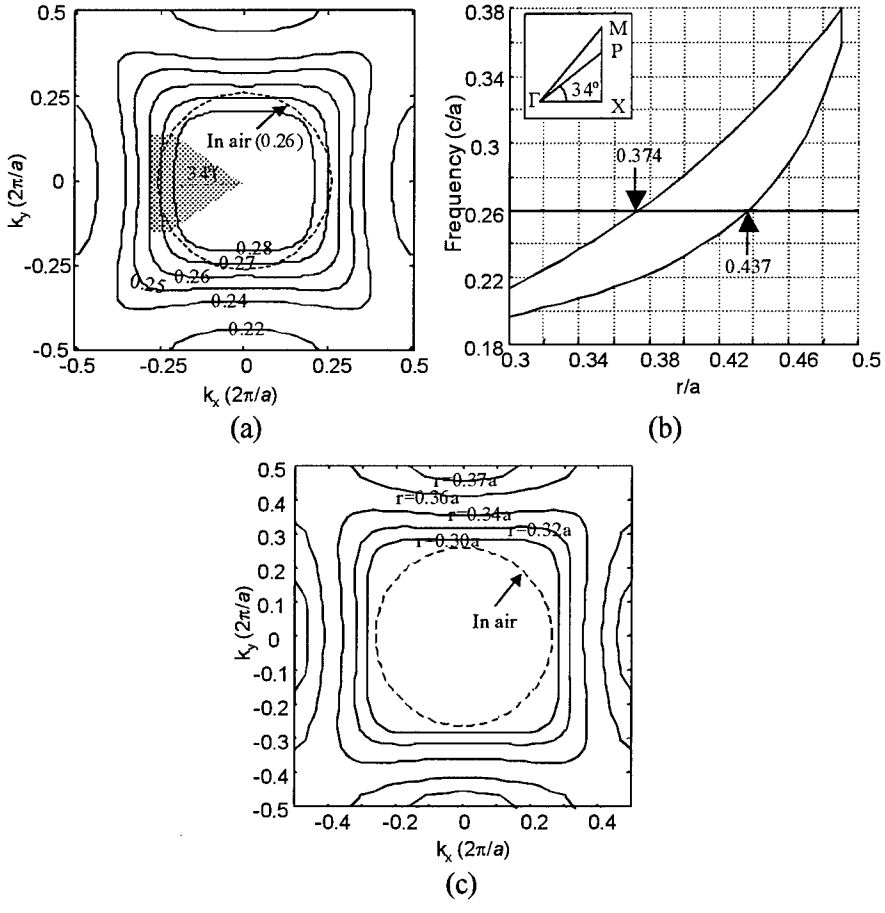

Figure 13: (a) Equi-frequency contours for the second band with radius of air hole of $0.3a$, (b) Stop band map for square lattice as radius of air holes vary, (c) Equal-frequency contours at frequency $0.26c/a$ with different radius of air hole

Due to the complexity of the electromagnetic interaction within this compact beam-splitting structure, a numerical method, namely the Finite-difference and Time-domain (FDTD) method [9], is applied to analyze this device. Figure 12 shows a three-layer PhC splitting structure formed by varying the hole radii in the outlined diagonal region. An incident Gaussian beam of width $2a$ is excited from port 0 and propagates through the dispersion guiding structure, splitting into two beams between ports 1 and 2. The steady state results are stored to calculate the power flow vectors in the x and y directions. The energy can then be calculated by integrating the power passing through a window of width $w = 5a$ as shown in Fig. 12 at port 1 and 2.

If the radius of air holes in the splitting region is equal to those in the dispersion guiding structure, it is clear that the wave will completely output to port 1. This output energy, in fact, is used as reference value for splitting ratio calculations. Figure 14(a) shows the steady state result

of the magnetic field (Hz) for a hole radius of $0.42a$ in the splitting structure, displaying most of the energy exiting at port 2. When $r_s = 0.36a$, one obtains approximately 3-dB splitting, and the corresponding steady state result of the magnetic field is shown in Fig. 14(b).

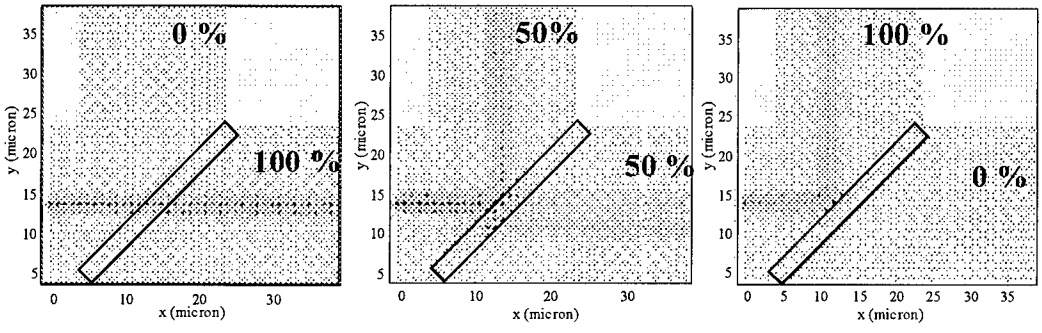

Figure 14: Three-steady state snapshots of the structure shown in Fig. 12 with various split ratios between port 1 and port 2

By varying the radius continually from $0.3a$ to $0.435a$, we calculate the percentage of optical power versus the normalized radius as shown in Fig. 4. At a radius of $0.36a$, the output ports have nearly the same power. Within the radius range $(0.3a < r < 0.345a)$, there is no stop band. As such, the EFC at frequency $0.26c/a$ is still square-like in shape; however, a majority of the light will propagate in the same direction as the incident wave with a small amount entering port 2 due to the interface of the two slightly different types of PhC structures. As the radii of air holes continue to increase, the frequency $0.26c/a$ falls into the band gap. However, as we mentioned above, since the frequency is close to edge of the band gap, a few PhC layers are not sufficient to completely reflect the light, and a portion of the signal will output to port 1. As we can see from Fig. 15, the power variation between the two output ports occurs within the stop band. For r_s between $0.3a$ and $0.435a$, the total output power is between 80% and 100%, where the loss is due to scattering from the splitting structure.

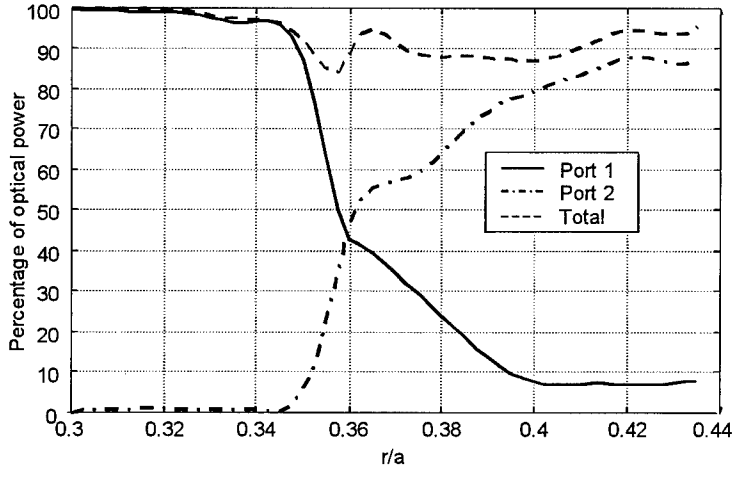

Figure 15: Percentages of output optical power of port1 and port 2 vary with the radius of air holes of splitting structure.

4.1.2.2 Prototype Fabrication of a Single Splitter Unit

The three common PBG fabrication processes based on silicon on insulator (SOI) methods are electron beam lithography (EBL), interferometry, and self-assembly techniques. In Phase II, we concentrated on EBL on SOI technology as it is based on the well-established methods of the semiconductor industry and offers the best potential for small feature sizes and large volume production. SOI is an attractive platform for realizing dielectric waveguides and photonic band gap devices due to the large refractive index contrast between the silicon waveguide and the underlying SiO_2 layer. The refractive index contrast is necessary to confine light in the plane of the photonic crystal lattice and to realize a photonic band gap for lateral confinement in the waveguides. In Phase II, we fabricated devices that follow the processing steps shown in Figure 16.

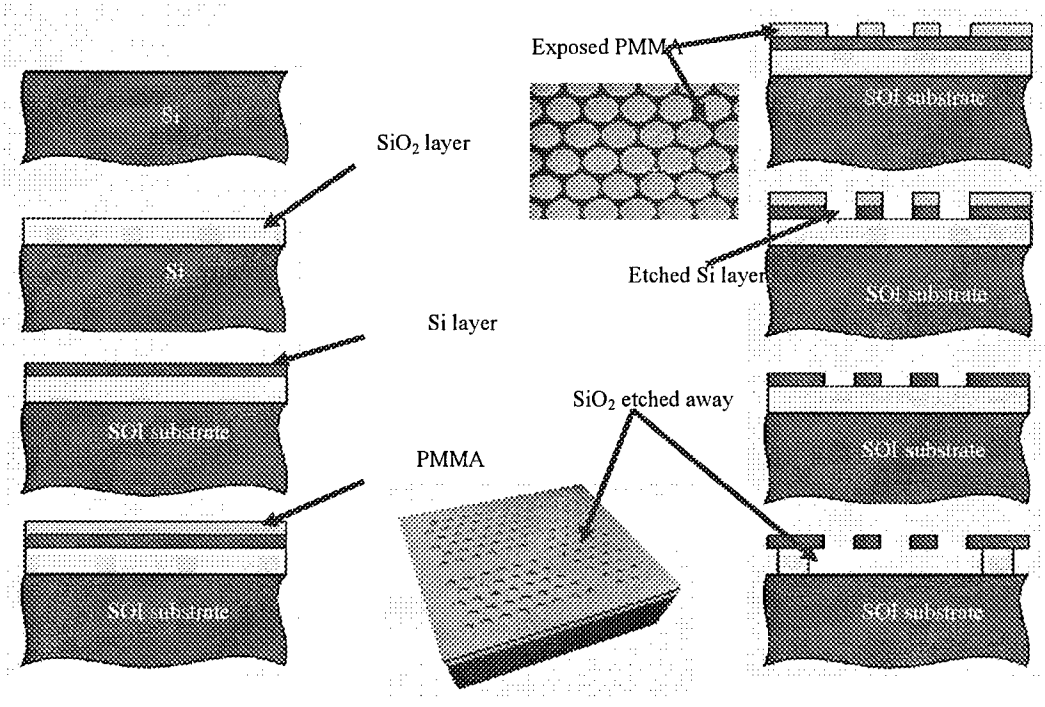

Figure 16: Silicon On Insulator Fabrication Process.

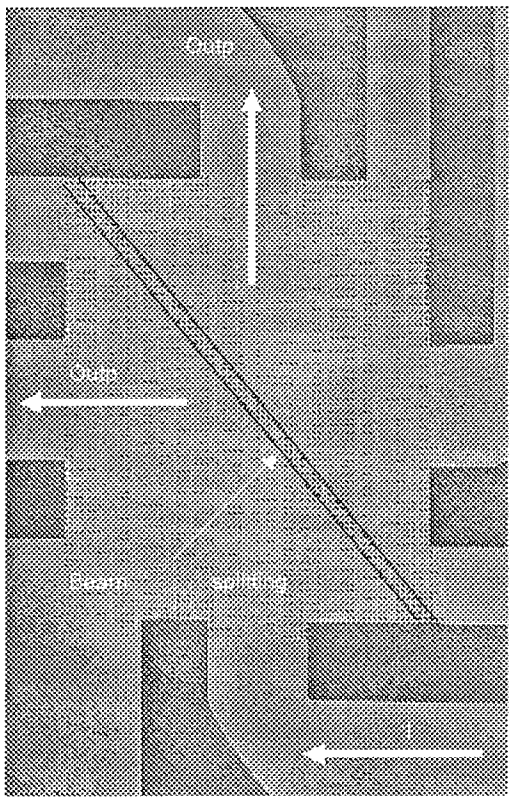

Figure 17: a fabricated prototype for the variable beam splitter structure shown in Fig 12

In this process a SiO_2 layer is deposited on a blank silicon wafer. Next, a layer of silicon is bonded to the SiO_2. PMMA is spun on the substrate and is used as an electron sensitive resist. Utilizing the unparalleled resolution of electron beam (e-beam) lithography, the PMMA is exposed and developed. Reactive Ion Etching (RIE) is then used to transfer the pattern to the silicon layer. In this step, it is important that the cylindrical structures that make up the PBG are etched with a high degree on anisotropy. To this end, the University of Delaware has developed a Bosch-like etching process that produces devices with straight walls and high aspect ratios. This process consists of a three step etching cycle, which is repeated a number of times to achieve the desired etch depth. First, a sidewall passivating polymer film is deposited using CF_4 and H_2 gases. The deposition is followed by two etch steps that use a mixture of SF_6 and He gases. The passivating film prevents the Si sidewalls from being isotropically etched by the SF_6 discharge, which contains a large concentration of atomic Fluorine. During the subsequent etch step, 'the smash,' the passivating polymer film is preferentially removed from the bottom of the trenches due to hard ion bombardment in a SF_6 and He plasma. In the second etching step, the SF_6 and He plasma, containing a large concentration of atomic Fluorine, etches the silicon in the preferred downward direction, while the passivating polymer prevents sidewall etching. The experimental variables that were optimized to arrive at the custom etch recipe included RF power, etch time, smash time, gas composition, etch pressure, deposition time, gas flow rates, and chamber conditions. This custom technique provides high selectivity, largely vertical sidewalls, and repeatability. Following the RIE step, SiO2 layer below the silicon PBG is etched away.

In Figure 17, we show the fabrication results for dispersion based variable beam splitter combing both a PBG and PhC structures. A J coupler is fabricated at the input and the output ports of the structure to facilitate efficient coupling form a conventional dielectric waveguide to the PhC structure.

Preliminary testing of the device is shown in Fig. 18, which is shown to be in agreement with our previously presented numerical results shown in Fig. 13, where we were able to experimentally validate the three cases presented numerically.

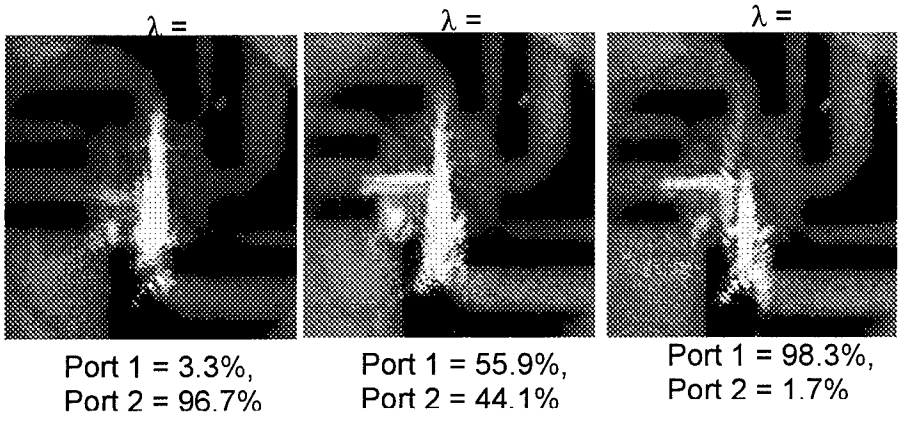

Figure 18: experimental validation for the variable beam splitter structure shown in Fig 13

4.1.2.3 Design of Multiple Splitting Units

With this self-guiding lattice, we proceed to design three beam splitters in order to separate optical signals. To do this, we increase the radius of one row of air holes along the Γ-M direction from $0.25a$ to $0.4a$, as shown in Fig. 19(b) and (c). This perturbation breaks the uniformity of the self-guiding PhC lattice. Therefore, when the self-guiding beam propagating along the Γ-X1 direction hits the perturbed air holes, part of it redirects from the original Γ-X1 direction to the Γ-X2 direction while the other part remains on its original propagation path. To demonstrate this, we launched a Gaussian beam into this perturbed self-guiding lattice along the Γ-X1 direction and simulate the propagation of the Gaussian beam in the lattice using the FDTD method. Figure 19(b) shows the simulation results, which clearly indicates the splitting of the self-guiding beams by the perturbed air holes. In this case, there is 26% of power in the coming self-guiding beam transmitted to port I and the other 74% redirected to port II. Moreover, when we increase the radius of the perturbing air holes to $0.45a$, the majority of power (around 93%) is redirected to Port II. Figure 19(c) shows the simulation result for this case. To systematically investigate the effect of the size of the perturbed air holes on the splitting ratio, we vary the radius of the perturbed air holes from $0.25a$ to $0.46a$ and calculate the power at Port I and II for each case. Figure 20 plots the relative output power at port I, II and their sum verse the radius of the perturbed air holes. From this figure, one can see that when the radius of the perturbed air holes is $0.25a$, the lattice is unperturbed and all incident power is transmitted to Port I. When it is $0.46a$, all power is redirected to Port II. The other splitting ratio can be achieved by adjusting the size of perturbing air holes in between.

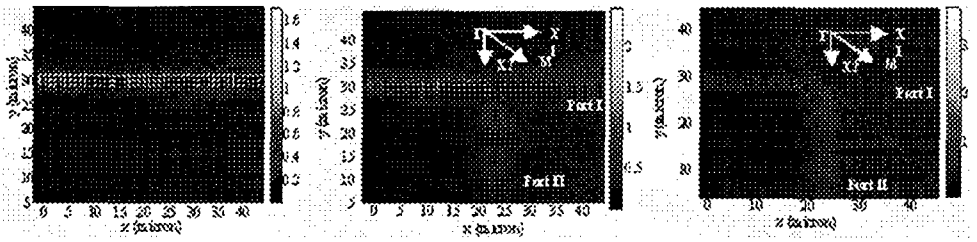

(a) (b) (c)

Figure 19: (a) Beam propagation in a self-guiding lattice, (b) splitting self-guiding beam when the radius of the perturbed air holes is 0.4a, (c) reflecting self-guiding beam when the radius of the perturbed air holes is 0.45a.

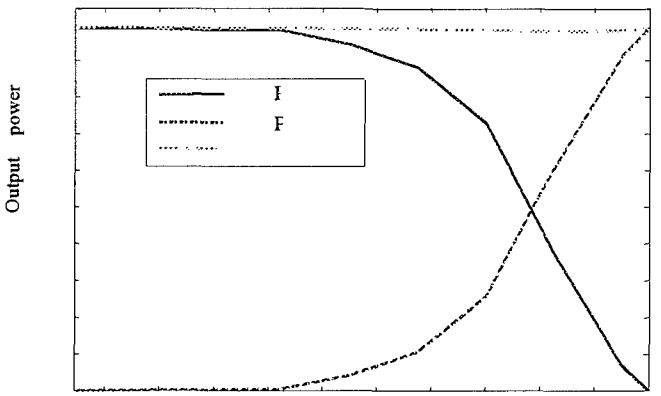

Figure 20: Plot of output power verse radius of the perturbed air holes.

4.1.2.4 Fabrication of the Multiple Splitting Units

To experimentally validate the design concepts multiple splitting units, we first fabricated the self-guiding lattice on a silicon-on-insulation (SOI) wafer, which has 260nm-thick silicon device layer on a 1μm-thick SiO2 insulating layer. E-beam lithography and inductively coupled plasma (ICP) dry etching was employed to pattern and transfer the structure to the silicon device layer. The underneath SiO2 layer was removed using buffered oxide etching (BOE). Figure 21 shows SEM micrographs of fabricated splitters. The self-guiding region of splitters consists of a square array of air holes. The radius of air holes is 220 nm and the lattice constant a is 450 nm. The splitters are diagonal rows of air holes with different radius from self-guiding region. A tapered dielectric waveguide was used to couple the input light into the self-guiding beam to control the beam width. Since the self-guiding lattice automatically collimates the input beam with an angular spectrum in a wide region, the tapered input waveguide does not affect the operation of the device. To test these fabricated splitters, the sample was cleaved and light from tunable laser was coupled onto the input facet of a tapered dielectric waveguide by a tapered polarization maintained fiber. The tapered waveguide is interfaced with the self-guiding lattice along the Γ-X1 direction. When the wide beam from fiber is narrowed down by the tapered waveguide, it is self-collimated and guided by the PhC lattice along the Γ-X2 direction. A narrow self-guiding beam is beneficial to high-density integration. When the self-guiding beam propagates through

the uniform lattice and arrives at the splitting structure, it splits to the transmitted light and the reflected light. The splitting ratio varies with the size of air holes of the splitting structure. Figure 7 demonstrates this behavior, where (a) is the top-down images captured by an IR CCD camera for the case with the radius of the splitting structure of 368 nm at the wavelength of 1560 nm. In contrast to the normally observed radiating light guiding path in the case of PhC band gap line defect waveguide [12], the self-guiding path is absent of any observable light, which indicates low radiation loss due to the fact that the selected mode region falls outside the light cone, as illustrated above. However, due to the break up of the lattice uniformity, the perturbed splitting air holes cause some radiation loss, as observed and indicated by a circle in Fig. 22(a). On the other hand, the fact that only a narrow part of the splitting structure is radiating, which shows that the propagating beam is well confined laterally by the self-guiding lattice. The large bright spot at right hand side is the scattered light at the intersection between the dielectric waveguide and the self-guiding PhC lattice, which might be caused by the discontinuity of the effective index between two materials and could be improved using adiabatic structure. To characterize the relation between the splitting ratio and the size of splitting air holes, we further varied the radius of splitting air holes and measured the output powers for each case. Figure 22(b) is the resulted plot, which again shows that the output power at port I decrease as the radius of splitting air holes increases while the opposite is true for Port II. Due to the unknown coupling losses from the laser output to the fiber, then to the dielectric waveguide, and finally to the self-guiding lattice in the experiment, we normalized the output power at each port to the total output power to eliminate the influence of these losses as well as the scattering loss in the splitting region on the characterization of splitting ratios.

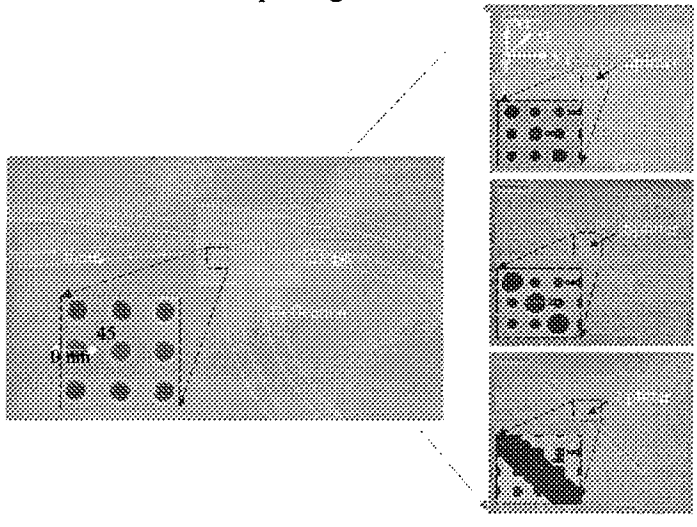

Figure 21: SEM pictures of three of the fabricated self-guiding splitters.

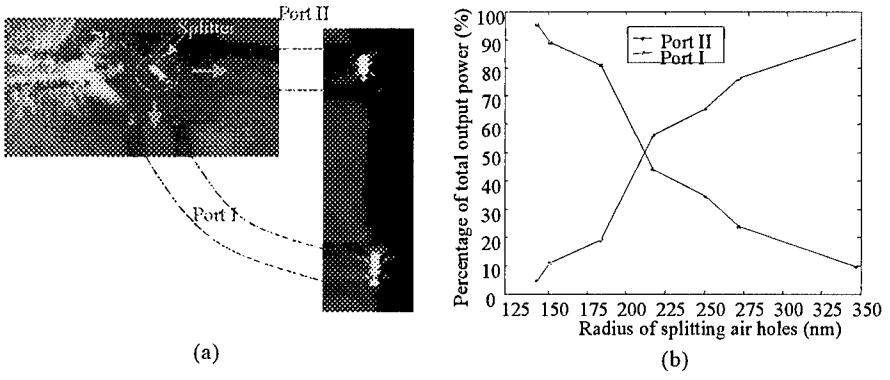

Figure 22: Characterization of self-guiding splitters: (a) the top-down images captured by an IR CCD camera for the case with the radius of the splitting structure of 368 nm at the wavelength of 1560 nm, (b) the measured relation between the output powers and the radius of splitting air holes.

4.1.3 Two-Bit All Optical Photonic Crystal Based ADC Implementation

Our first approach toward implementing a photonic crystal based optical analog to digital converter is to combine a self-collimated photonic crystal waveguide structure with an array of splitters formed by etching a small slit. Varying the slit width controls the ratio of the transmitted/reflected beam through the various branches as shown in Fig. 23

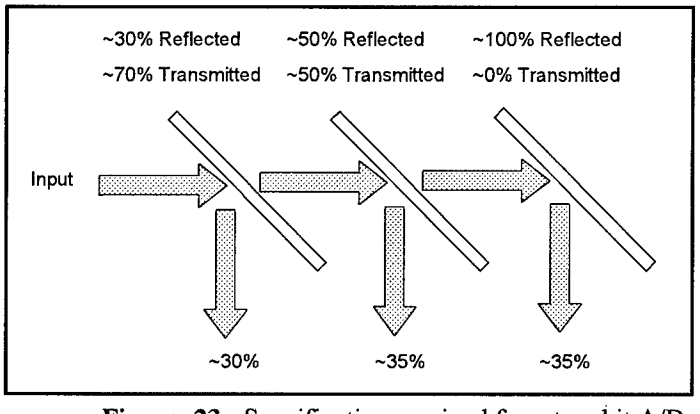

Figure 23: Specification received for a two bit A/D

Prior to exciting the structure with a monochromatic light wave at the input port, careful study of the relationship between slit width and splitting ratio was performed to determine the appropriate slit dimension to provide the performance expected of each branch. To do so consider the structure shown in Fig.24. In an absence of a slit structure an incident light beam incident through the input port will be self-collimated through the photonic crystal structure and will exit at the output port I with no distortion. Once a slit structure is introduced, it will interact with the incident light beam through the input port as to divert part of the incident beam toward output port II and allow the other part to exit at port I. the width of the slit structure determines the proportion of the light exiting at port I versus that exiting at port II. If the slit structure is wide enough, it will act as a reflecting mirror in which case, the incident light will completely

diverted to port II. We identified this to be a threshold value of the slit structure and referred to it as $W_{threshold}$. Hence any slit width equal to of greater than $W_{threshold}$ will completely reflect the incident light to exit at port II. While for values of ($0 < W_{Slit} < W_{threshold}$) partial splitting will occur.

For a silicon based photonic crystal self-collimated waveguide structure with an air hole radius to lattice constant ratio of 0.3 and a lattice constant of 0.26λ, we varied the width of the slit structure and measured the percentage of the transmitted versus reflected wave at 1500nm as shown in Fig. 25

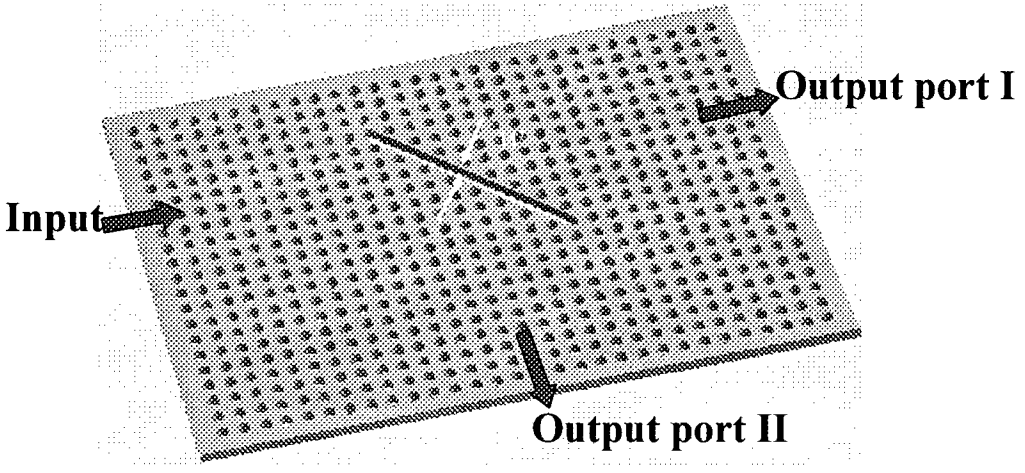

Figure 24: A slit structure of width W combined with a self-collimated Photonic crystal structure.

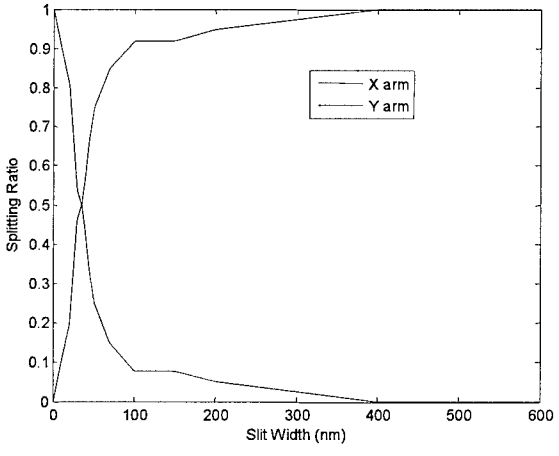

Figure 25: Slit width versus splitting ratio

Based on the spectral results shown in Fig. 25 we proceeded to design the three splitters shown in Fig. 23. For the first splitter with 70% transmission and 30% reflection we used a slit

with a width equal to 25nm, for the 2nd splitter with 50% transmission and 50% reflection we used a slit width equal to 35 nm, and for the 3rd splitter with 0% transmission and 100% reflection we used a slit width equal to 400nm. The steady state results for the various splitters is shown in Fig. 26.

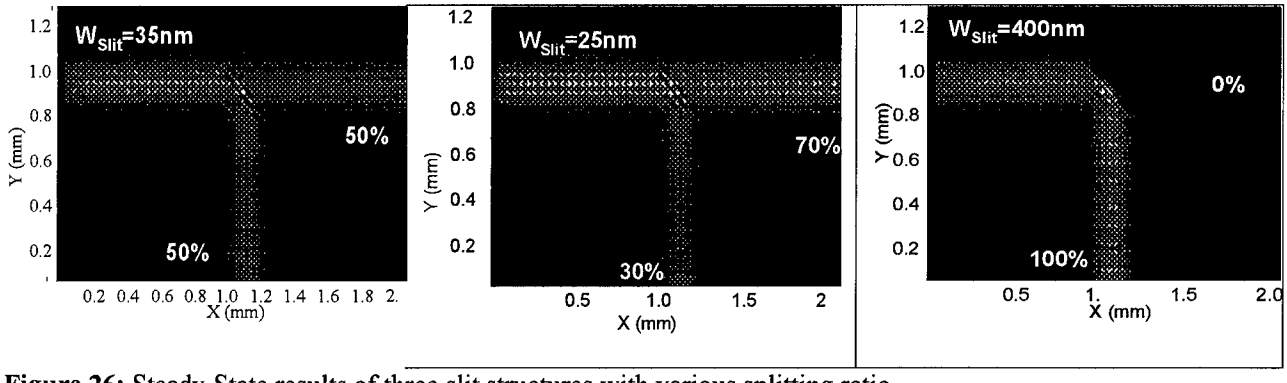

Figure 26: Steady State results of three slit structures with various splitting ratio

The results shown in Fig.26 was also combined together to construct a two-bit A/D converter shown in Fig 27 (a)

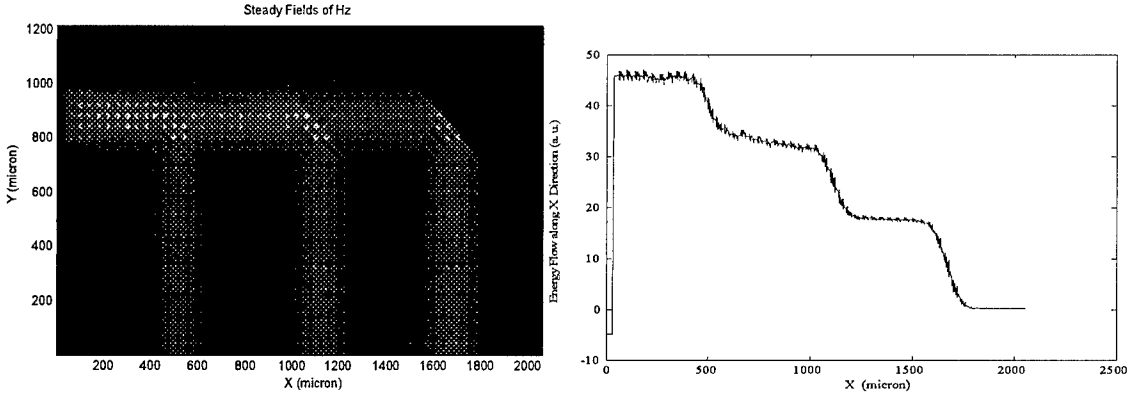

(a) (b)

Figure 27: Simulation result of a 2 bit A/D structure along with calculated energy flow through the structure

The energy flow along the x direction was also calculated and plotted in Fig.19(b)

4.1.3.1 Experimental Demonstration of the Two-Bit ADC

To experimentally validate the design concepts of the 2-bit optical A/D converter, we first fabricated the self-guiding lattice on a silicon-on-insulation (SOI) wafer, which has 260nm-thick silicon device layer on a 1μm-thick SiO_2 insulating layer. E-beam lithography and inductively coupled plasma (ICP) dry etching was employed to pattern and transfer the structure to the silicon device layer. The underneath SiO_2 layer was removed using buffered oxide etching

(BOE). Figure 28 shows SEM micrographs of fabricated splitters. The self-guiding region of splitters consists of a square array of air holes. The radius of air holes is 220 *nm* and the lattice constant *a* is 450 *nm*. The splitters are diagonal rows of air holes with different radius from self-guiding region. To test these fabricated splitters, the sample was cleaved and light from tunable laser was coupled onto the input facet of a tapered dielectric waveguide by a tapered polarization maintained fiber. The tapered waveguide is interfaced with the self-guiding lattice along the Γ-X1 direction. When the wide beam from fiber is narrowed down by the tapered waveguide, it is self-collimated and guided by the PhC lattice along the Γ-X2 direction.

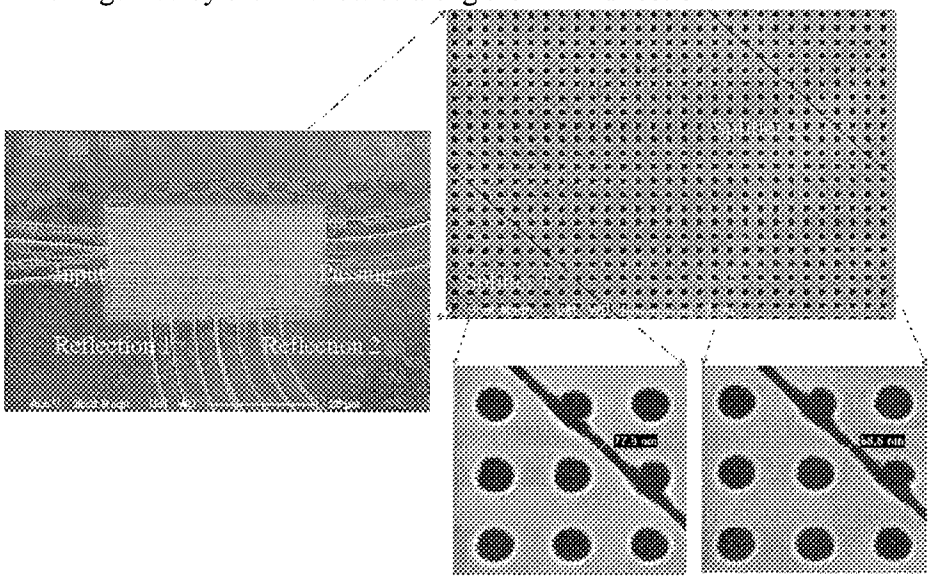

Figure 28: A Fabricated Two bit A/D prototype

A narrow self-guiding beam is beneficial to high-density integration. When the self-guiding beam propagates through the uniform lattice and arrives at the splitting structure, it splits between a transmitted light and the reflected light. The splitting ratio varies with the size of air holes of the splitting structure. Figure 29 demonstrates this behavior, where (a) is the top-down images captured by an IR CCD camera for the case with the radius of the splitting structure of 368 nm at the wavelength of 1560 nm. In contrary to the normally observed enlightened light guiding path in the case of PhC band gap line defect waveguide, the self-guiding path is absent of any observable light, which indicates low radiation loss due to the fact that the selected mode region falls outside the light cone as illustrated above.

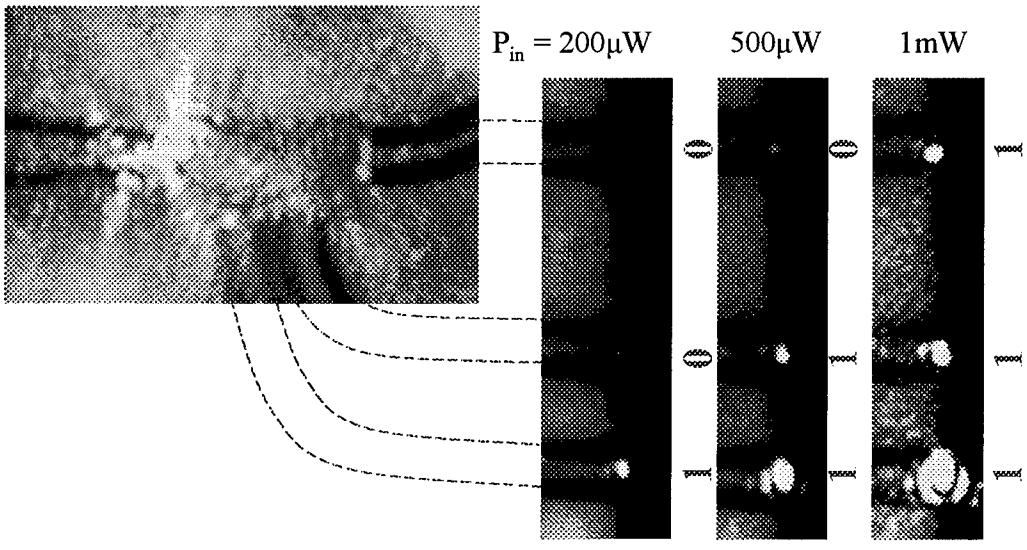

Figure 29: Experimental Characterization of the two bit A/D shown in Fig 28

However, due to the break up of the lattice uniformity, the perturbed splitting air holes cause some radiation loss, as observed in Fig.**29**(a). On the other hand, the fact that only a narrow part of the splitting structure is enlightened shows that the propagating beam is well confined laterally by the self-guiding lattice. The large bright spot at the left hand side is the scattered light at the intersection between the dielectric waveguide and the self-guiding PhC lattice, which might be caused by the discontinuity of the effective index between two materials and could be improved using adiabatic structure.

4.1.3.2 Implementation of 3 bit ADC

Examining the transmission of the slit width shown in Fig.28 one can observe that the operating range of slit width(s) is relatively narrow. In order to implement a 3 bit A/D we will need 7 splitters. In order to enlarge the operating dynamic range shown in Fig. 25 we replaced the slit structure with a single PhC layer operating in the stop band as shown in Fig 30.

By varying the fill ratio of the air hole in the PhC splitting layer we can precisely control the transmission/reflection ratio and hence enhance the operating dynamic range of the splitting structure. Using our FDTD based tools developed in house, we performed an extensive analysis of various ratios of air hole in the splitting region and we measured the percentage output power between the through port and the reflection port in each case. A summary of this analysis is shown in figure 31, which shows the steady state results for a single monochromatic incident wave with wavelength 1500nm and using a TE polarized wave.

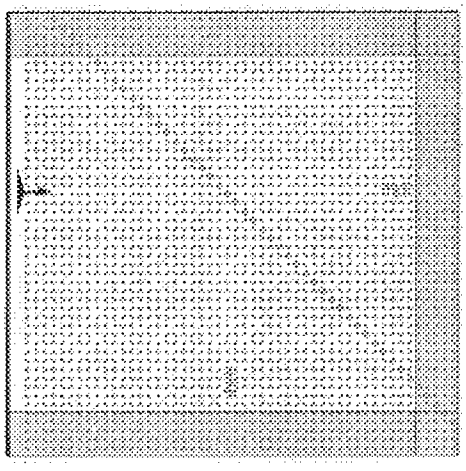

Figure 30: PBG based implementation of a single splitter unit

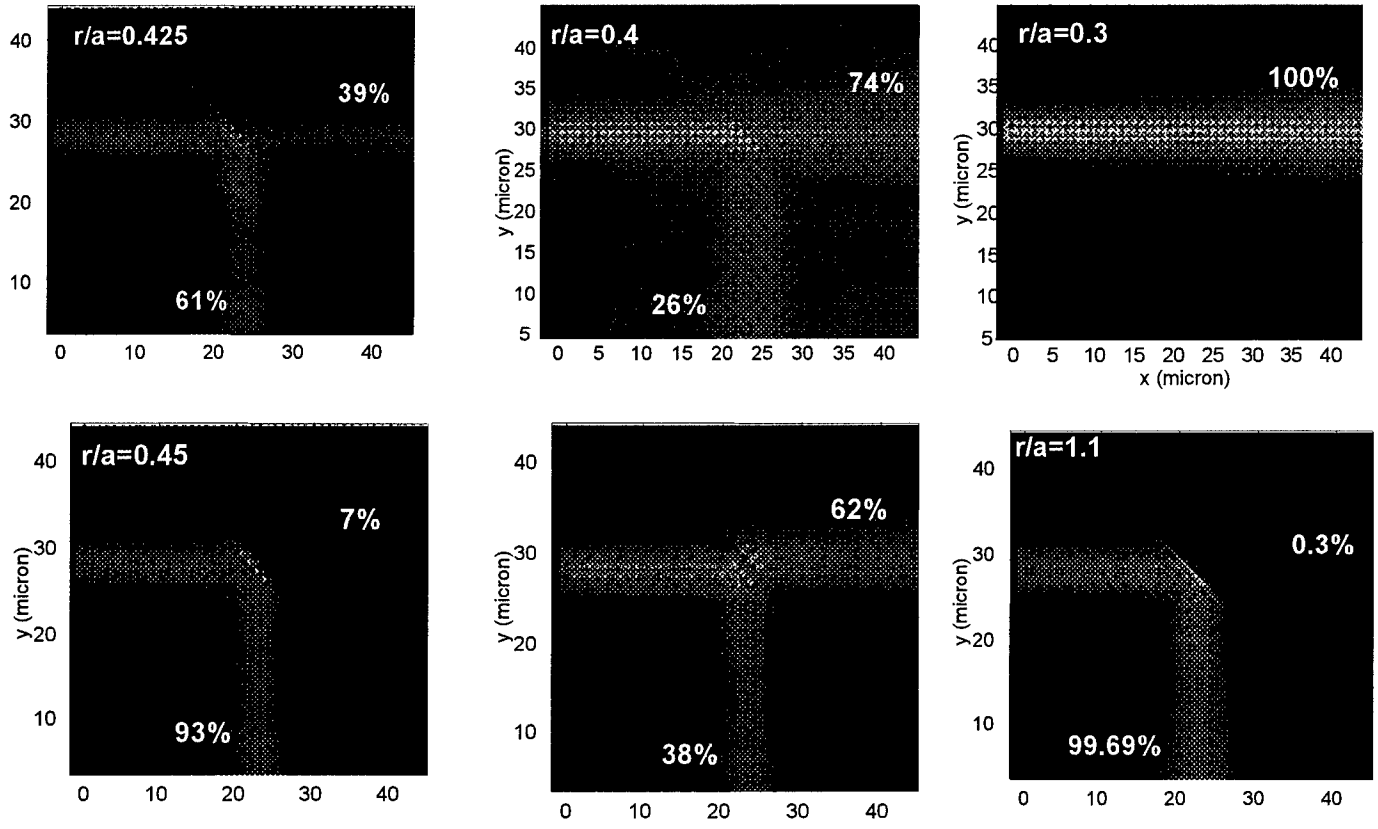

Figure 31: Steady state results for PBG based splitters of various air hole to lattice constant ratios were shown to provide variable splitting ratios

FDTD results shown in Figure 31 are summarized in Fig 32

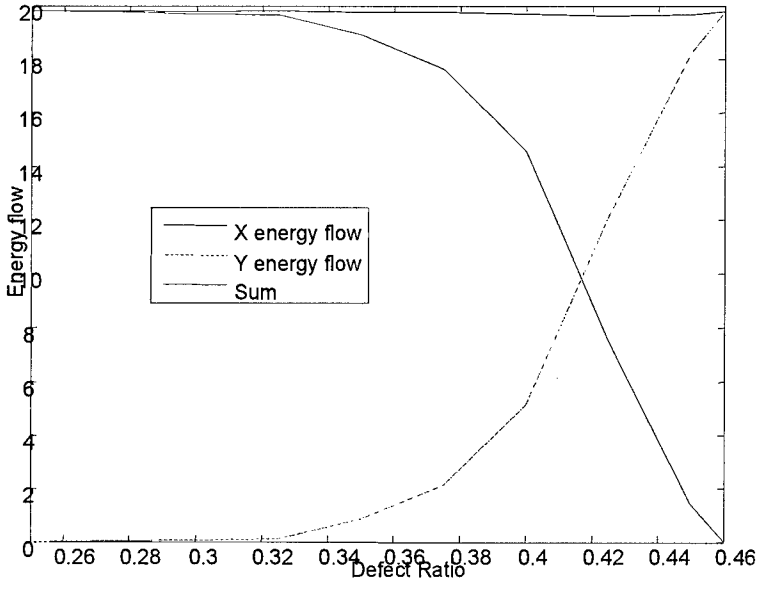

Figure 32: Relationship between defect ration in the splitting region versus energy flow between through and reflection ports

Based on the results shown in Fig. 32 we constructed a 3 bit A/D consisting of 6 splitters and a through pass as shown in Fig. 33.

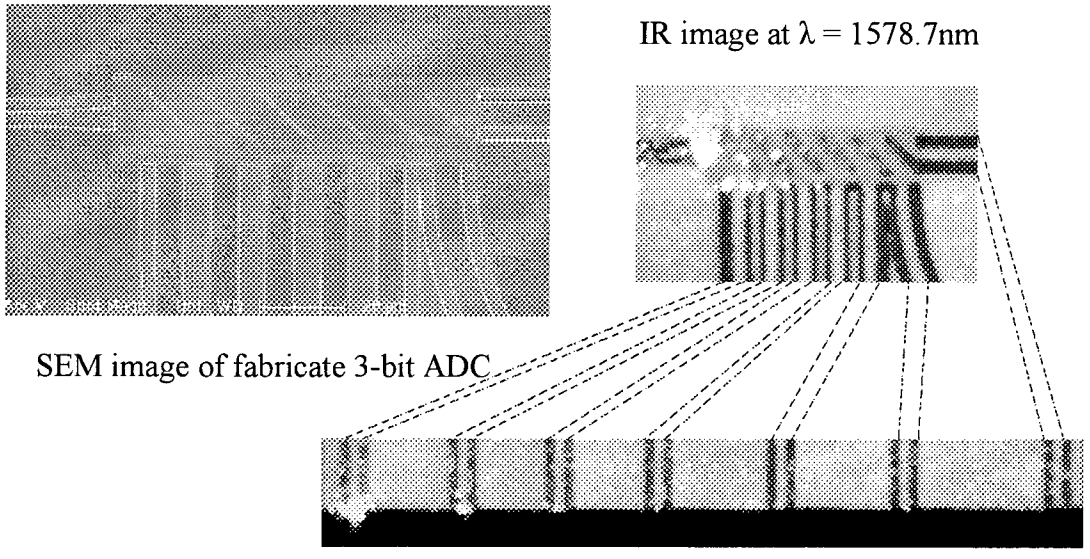

Figure 33: A fabricated and characterized six PBG based splitters designed to perform as a 3 bit A/D

4.2 Part II: Photonic Crystal Based Multi-Spectral Receiver

On December 8th , 2004, a 2nd kick-off meeting was held at EM Photonics, in attendance were, Dr. Walter Buckwald, representing Dr Richard Soref, AFRL/SNHC Dr. Dennis Prather, University of Delaware and Dr. Ahmed Sharkawy, Mr. Eric Kelmelis EM Photonics, Inc. During the course of the meeting, Dr. Prather led a tour of current university of Delaware lab facilities and equipments which can befint the AFRL during the course of this. Mr Kelmelis presented an overview of projects at EMP, Dr Sharkawy presented current progress and highlighted the objectives of the current STTR Phase II program.

During the effort of Phase I, Dr. Soref proposed a "Multi-Spectral Receiver" (MSR) shown in Figure 34,

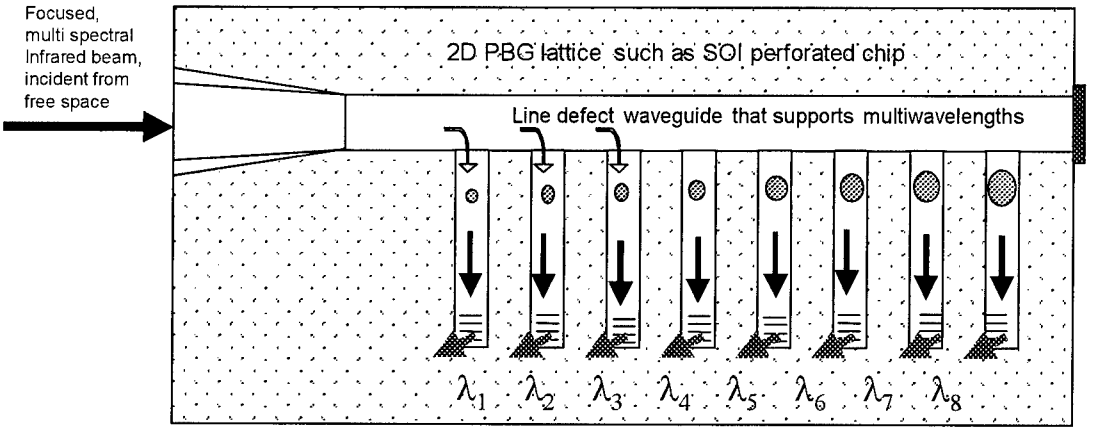

Figure 34: A multi-Spectral Receiver

In this application, a multi-spectral infrared beam is launched in a PBG waveguide that supports the wavelengths of interest. Resonators are used for filtering individual wavelengths into separate guides. The entire silicon wafer is bonded to a detector array, thereby monitoring each wavelength independently. Dr. Soref mentioned that a suitable detector array is also under development at AFRL.

As previously described, the Multi-Spectral Receiver is based on a PBG waveguide that supports the wavelengths of interest. Resonators are used for filtering individual wavelengths into separate guides. In Figure 35, a silicon and air hole lattice is represented with a multi-spectral source (red arrow graphic) and a defect resonator for wavelength selection.

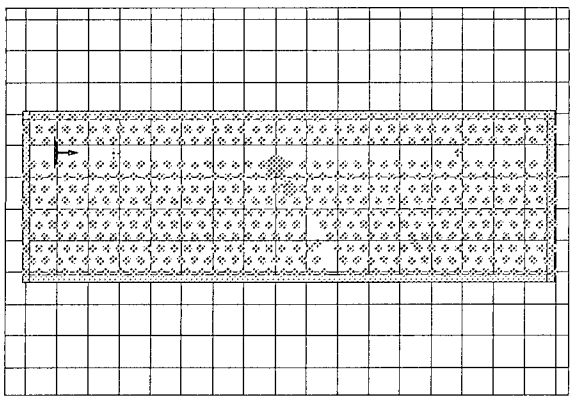

Figure 35: Wavelength Tap, Device Design

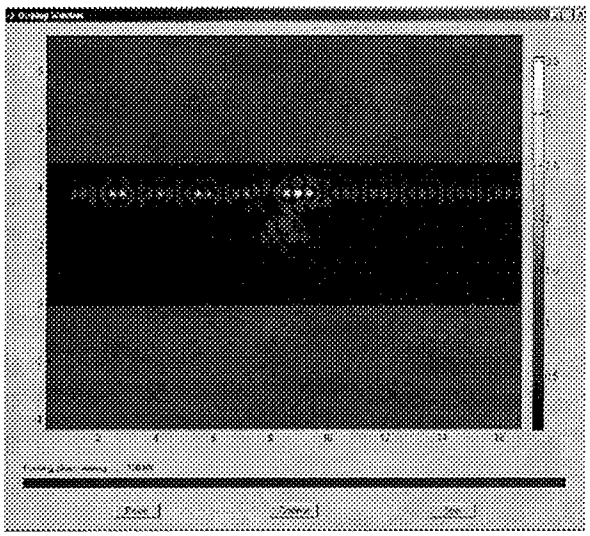

Figure 36: EMPLab^{TM} Simulation

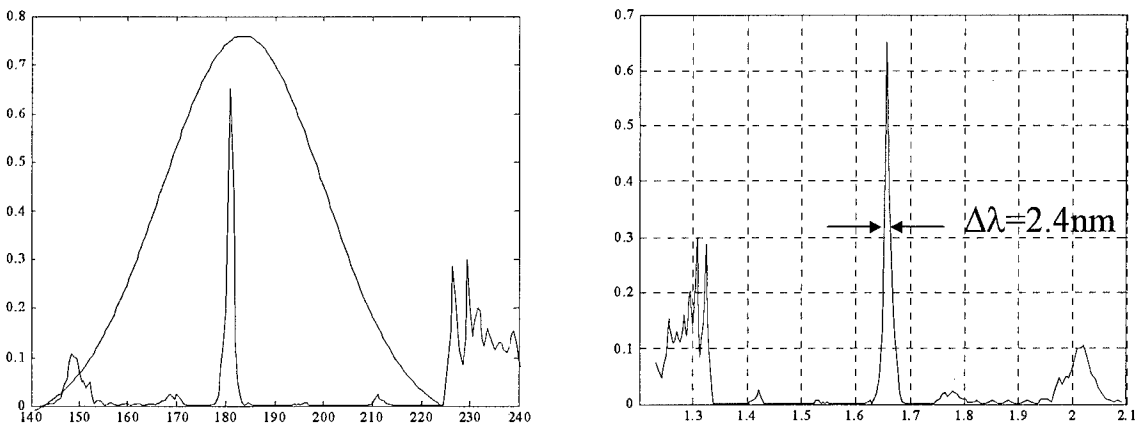

Figure 37: EMPLab^{TM} Results, a 2.4nm filter

Our analysis shows that over very large wavelength bands, filter taps can be fabricated that allow for better than 2.5 nm resolution which is appropriate for the MSR application.

In Figures 38 and 39, we show the fabrication results for the MSR system. A primary waveguide was fabricated that supports multiple wavelengths. Defects of various sizes were produced to measure wavelength filtering.

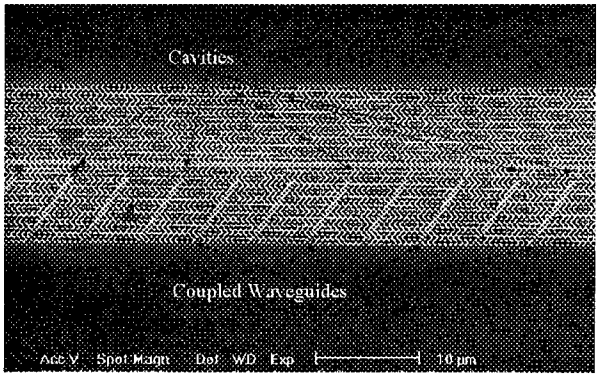

Figure 38: Defect -Tuned Channel Drops

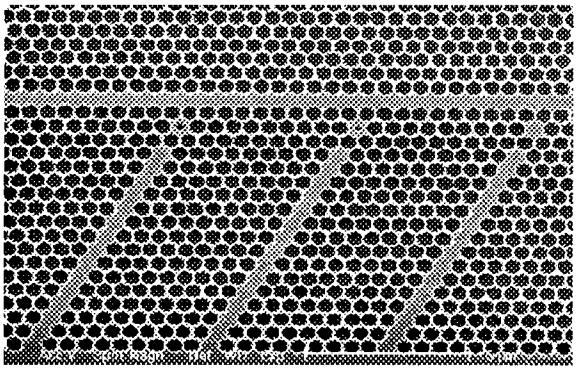

Figure 39: Defect -Tuned Channel Drops

Preliminary testing of this device indicated that due to tight tolerances, defects may have to be larger to achieve sufficient coupling into the tapped guides. Hence even though using point defect approach is ideal for attaining narrow band filtering, it is highly sensitive to fabrication tolerances which has to be within or less than 5%. Hence in search for another alternative which may not require as high fabrication tolerances, we collaborated with Dr Soref and came up with the structure shown in Fig. 40

The simulation and experimental results presented in Part I of this report can be further utilized to implement a static or a dynamic Multiple Spectral Receiver by examining the frequency response of each splitter or of an array of splitters over a wide frequency range. Such behavior can be further engineered to provide filtering as shown in Fig.40 below.

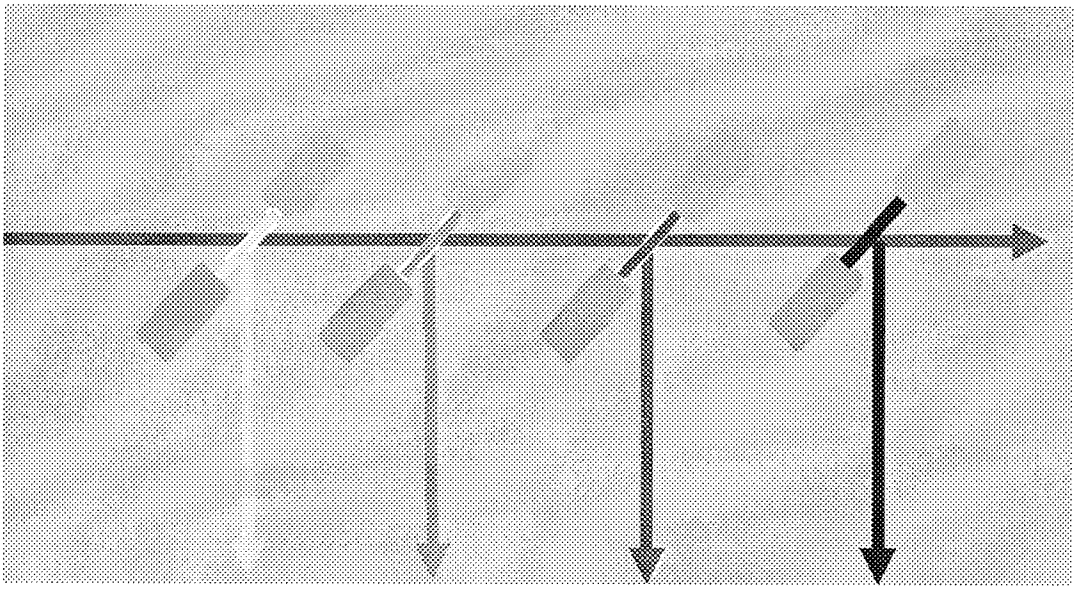

Figure 40: Utilizing the A/D design in part I to perform as a wide band frequency selective filter

Consider the structure consisting of 3 splitters shown in Fig. 41 if a broadband pulse is incident through the input channel, each splitter will respond to the various frequency content of the incident signal differently and hence temporal filtering can be attained, as shown in the experimental results shown in Fig. 42

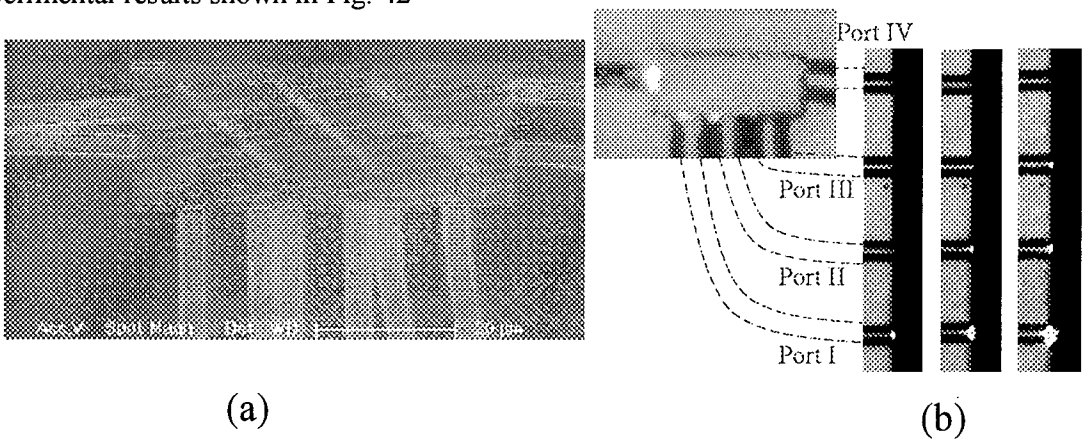

Figure 41: A 3 splitter A/D structure

From the results shown in Fig 42 we can see that by careful design and engineering of the properties of the various PBG splitter layer one can implement frequency selective filtering

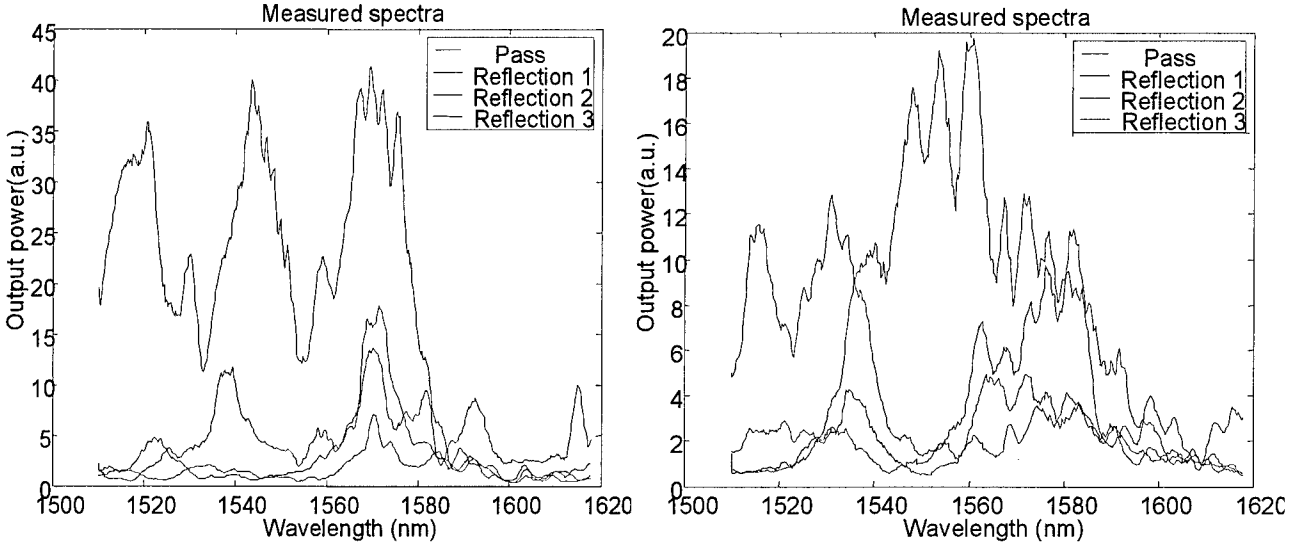

Figure 42: Transmission spectra measured experimentally for two different prototypes containing 3 splitters each

If the static splitters shown in Fig. 41 were to be replaced with PN or PIN junctions to create active splitters, additional more exciting functionalities can be further integrated within our A/D-MSR Photonic crystal based device. Additional functionalities include 2 by 4 and 4 by 4 optical switching. In addition the number of splitters necessary to implement an N-bit will be linearly proportional to the number of bits; i.e., 3 splitters will only be needed to implement 3 bit A/D instead of 8 splitters as in case of the static implementations. Also a reconfigurable switching

fabric can be also implemented. A concept device combining such functionalities is shown in Fig.43 and Fig. 44

Based on the achievements highlighted above EM Photonics put together a concept photonic crystal based device combining the general functionalities discussed above. The device represent a transparent self-collimation photonic crystal reconfigurable interconnect and is shown in Fig. 43 where Routing can be re-programmed by either electrically or optically inducing charge density that creates local reflecting mirrors within a self collimation photonic crystal . The device shown in Figure 43 combines both an ADC , MSR and an optical switching network as shown in Fig. 44

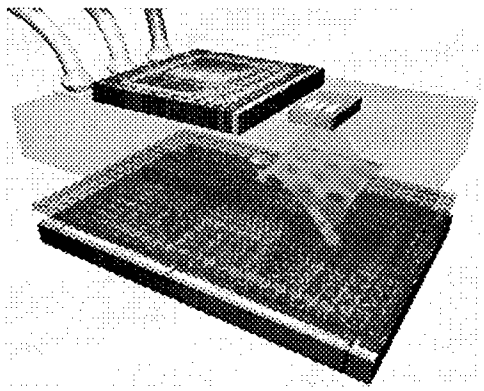

Figure 43: EM Photonics Self-collimation Photonic Crystal reconfigurable interconnect

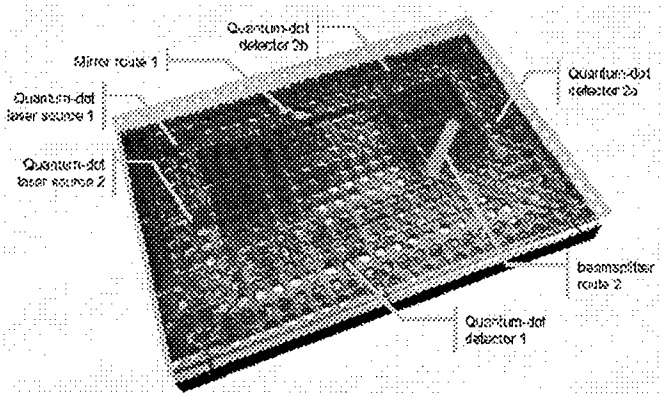

Figure 44:EM Photonics concept device for ADC, MSR and optical switching network

5 Phase II Results Summary

Our Phase II effort succeeded far beyond our expectations. We were able to design, model, fabricate and characterize novel photonic crystal devices to meet the technical specifications of multiple Air Force Research Lab groups. To summarize, we presented the first experimental demonstration an optical 2-bit A/D converter in a silicon photonic crystal structure. To do this, we first designed a self-guiding PhC lattice by using the iterative plane wave method to engineer a square like EFC. We then perturbed the uniform lattice at the three rows separated by a certain distance along the direction 45 degree to the self-guiding beam. In this way, three splitters were constructed in cascade, which results in three unique outputs of the device. Each splitter was designed to have a desired splitting ratio by adjusting the degree of its perturbation. Therefore, the three outputs reach the state '1' at different input power levels and we thus achieved four unique states '000', '001', '011', and '111' from the three output ports. By coding these four states into the desired four binary states '00', '01', '10', and '11', we were able to realize a 2-bit A/D converter. To experimentally validate these design concepts, we also fabricated and characterized the relation between the splitting ratio and the degree of the perturbation. Based on these understanding, we also proceeded to fabricate a 2-bit A/D converter consisting of three splitters and successfully characterized four unique states. It should be noted that the design concept discussed in this paper could be extended to A/D converter of a higher number of bits, although it requires finer adjustment of splitting ratio of each splitter and thus demands more precise fabrication control. In addition, we designed, modeled and fabricated a multi spectral receiver with a line width as narrow as 2.4nm which can be used for Dense Wavelength Division Multiplexing and filtering applications

In summary highlights of the Phase II technical achievements include

- Design of low resolution photonic crystal based A/D converter
  - Fabrication of designed prototypes
- Design of high resolution photonic crystal A/D converter using weighted tabs (slots)
  - Fabrication of designed prototypes
- Engineered dispersive properties of photonic crystals to implement a single splitting unit
  - Fabrication and characterization of the designed splitting unit
- Utilized dispersion based splitter to design an array of weighted photonic bandgap splitting units
  - Fabrication and characterization of designed prototypes
- Design of high resolution photonic crystal two bit A/D converter using 3 photonic bandgap splitting units
  - Fabrication and characterization of designed prototypes
- Design of high resolution three bit A/D converter using 7 photonic bandgap splitting units
  - Fabrication and characterization of designed prototypes
- Design of a photonic crystal based multisepctral receiver
  - Fabrication and characterization of designed prototypes
- Published 4 technical papers, presented 3 invited talks
- A patent is currently in process through AFOSR for various parts of this work

6 Commercialization

The overall objective of this STTR program is to *define and develop a unified manufacturing process for Photonic Band Gap (PBG) devices that combines design, simulation, fabrication, and test.* By investigating devices that serve the needs of current Air Force research programs, EM Photonics and the University of Delaware can achieve their technology transfer objectives and at the same time provide the most meaningful results to the Air Force.

With respect to the low cost fabrication procedure for nano structure based devices using chemical lithography, EM Photonics is uniquely qualified to commercialize this technology. This technology was highly endorsed with leading manufacturers of near field scanning optical microscopes and nanolithographic-based systems. EM Photonics will capitalize this endorsement and will work closer with those customers to integrate our current and future nanolithographic systems utilizing chemical lithography technology refined during phase I for next generation systems. EM Photonics will further purse other opportunities in physical and biological sciences and other micro-optic and Nano-MEMS technologies for chemical biosensors

6.1 Company

EM Photonics, Inc. is a small, high technology company that specializes in applications of micro and nano photonics technologies. Founded in August of 2001, EMP is privately owned and based in Newark, Delaware. Currently, EMP has 10 full time employees and 5 part time employees with expertise in optical system design, nano and micro-optical fabrication, and scientific computing. EMP maintains two locations, a facility with 1600 sq. ft of office and laboratory space and another facility with 800 sq. ft of sublet manufacturing space. Both of these facilities are within walking distance of the University of Delaware. EMP has 4 signed technology transfer agreements with the university and maintains a close collaborative relationship.

EMP receives revenue from consulting contracts to government and industry, fabrication services, and software sales. ***In 2005, EMP received 6 Phase I/II SBIR/STTR*** from different federal agencies, NIH, NSF, Department of Education, Office of Naval Research, Air Force Office of Scientific Research, and DARPA. These awards include the design and fabrication of optical components for applications such as biosensing, optical data storage, and spectroscopy. At this point, it is anticipated that EMP will have a solid foundation to expand its facilities and workforce, take on external investment for greater fabrication capability, and begin aggressive commercialization. Ultimately, EMP intends to become a full life cycle provider of various optical and microwave components for consumer, medical, and military applications. Our early success is evident in the following charts.

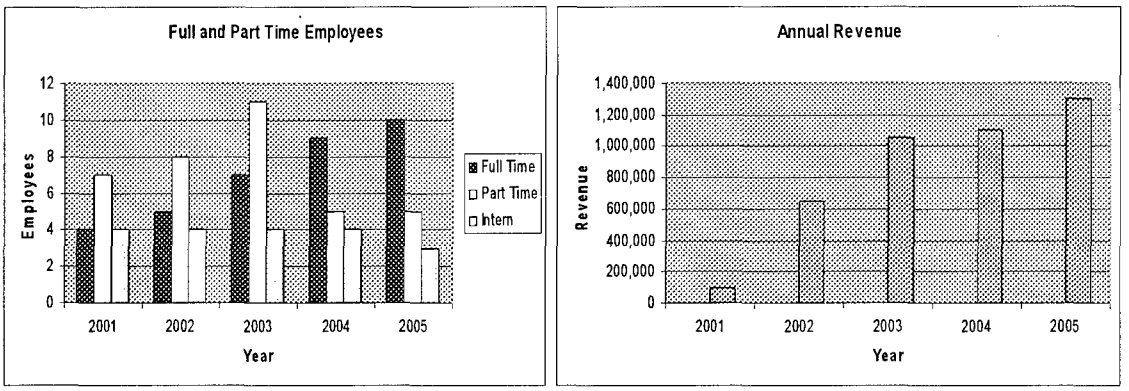

EM Photonics Growth

Growth of EM Photonics since it's founding in 2001.

The strength of our small business is exhibited in our ability to apply electromagnetic-base design technologies to a wide variety of applications. By understanding the requirements of our customers, we are able to develop tools and propose solutions that best suit their needs. Some of our projects from our first three years of business are shown below.

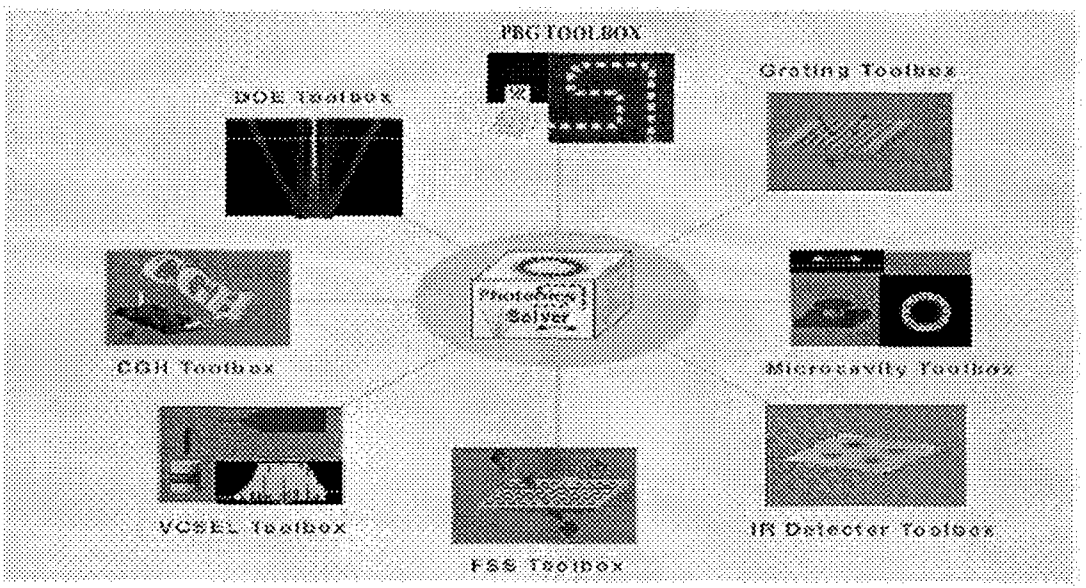

Commercial Launch of EMPLab Design and Simulation Software for Photonics

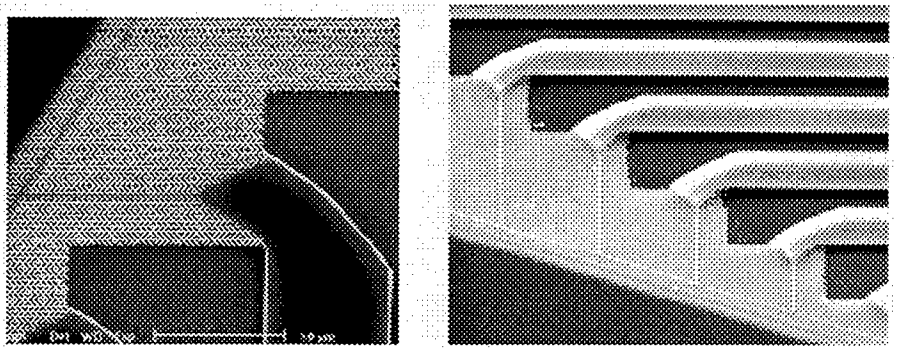

Photonic Crystal Design for Spectrum Analysis, Optical Data Storage, and Power Monitoring

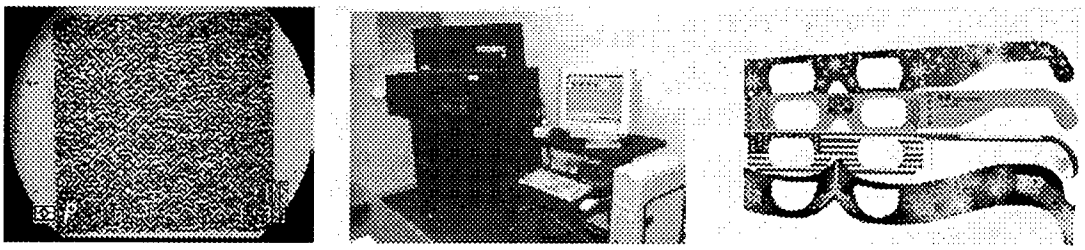

Direct Master Process for Novelty Holograms

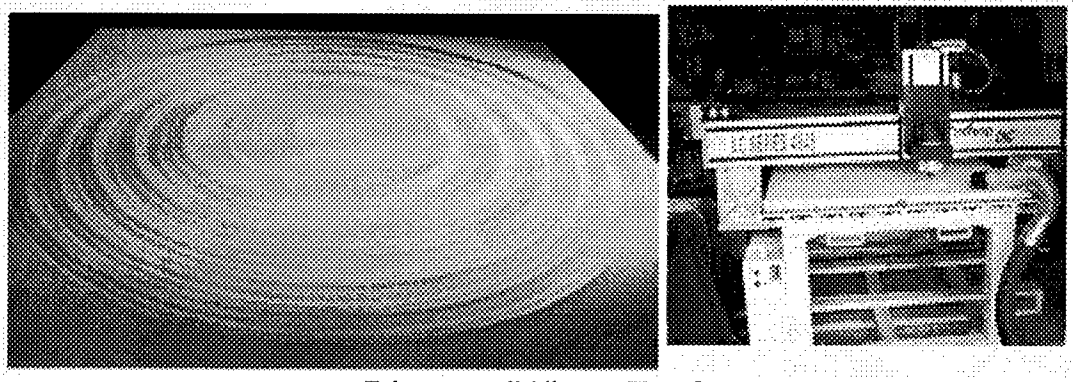

Fabrication of Millimeter Wave Optics

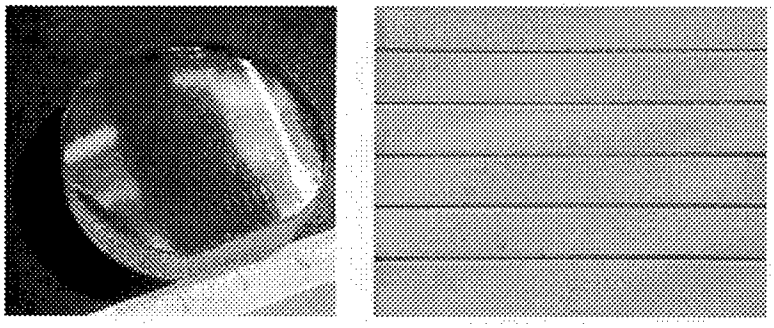

Complex Blazed Gratings for Spectroscopy

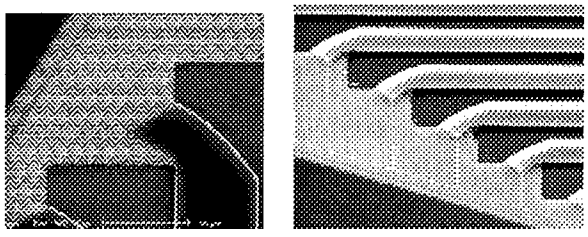

Photonic Crystal Devices for Spectrum Analysis, Optical Data Storage, Power Monitoring

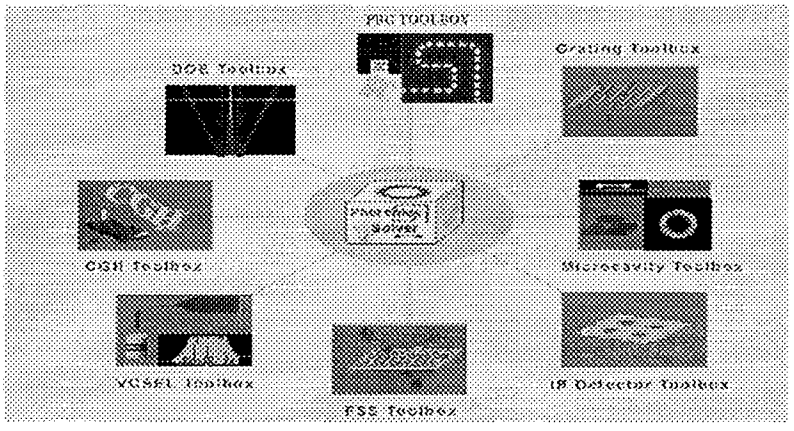

Commercial Launch of EMPLab, Design and Simulation Software for Photonics.

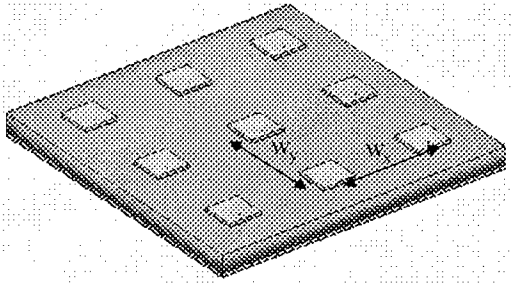

Phased Array Antennas on Large Area Substrates

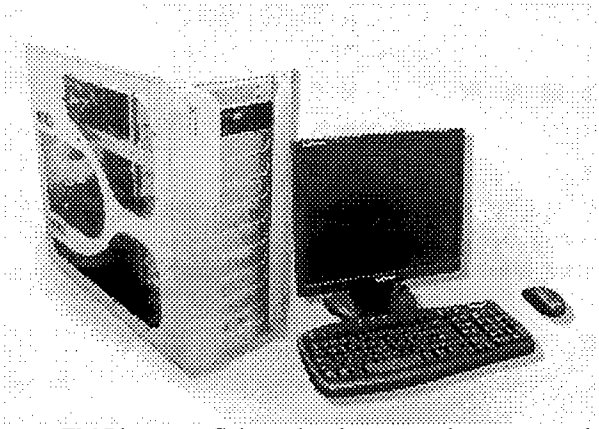

FDTD Workstation featuring EM Photonics Celerity hardware acceleration was developed under the SBIR program and is currently sold though Optiwave Systems.

6.2 Commercial Potential

A The global market for nanophotonic devices is projected to increase dramatically between 2004 and 2009-from $420 million to more than $9.3 billion-according to a soon-to-be-released report from Business Communications Company, Inc., Norwalk, Conn. Photonics, the technology of generating and controlling light, particularly to carry information, includes the emission, transmission, amplification, detection, modulation and switching of light. Nanophotonics involves the interaction of light with nanoscale structures and materials. Nanophotonic light-emitting diode (LED) technology, including flat-panel and plasma displays, accounted for more than 82% of the 2004 nanophotonics market. Near-field optics and nanocrystalline dye-sensitized solar cells accounted for 14.4% and 3.3%, respectively. LEDs is the fastest-growing nanophotonic market segment with a projected average annual growth rate of more than 90% between 2004 and 2009, reflecting their increased use in monitor and display applications. As this segment is projected to represent nearly 94% of the nanophotonics market by 2009, near-field optics and nanophotonic-integrated circuits (NPICs) are the only other device types expected to have market shares greater than 1%. The largest numbers, in terms of nanophotonic device sales, over the next five years are expected in the areas of monitors and displays, bioassays and computing and electronics, with lighting applications compromising a much smaller market share.

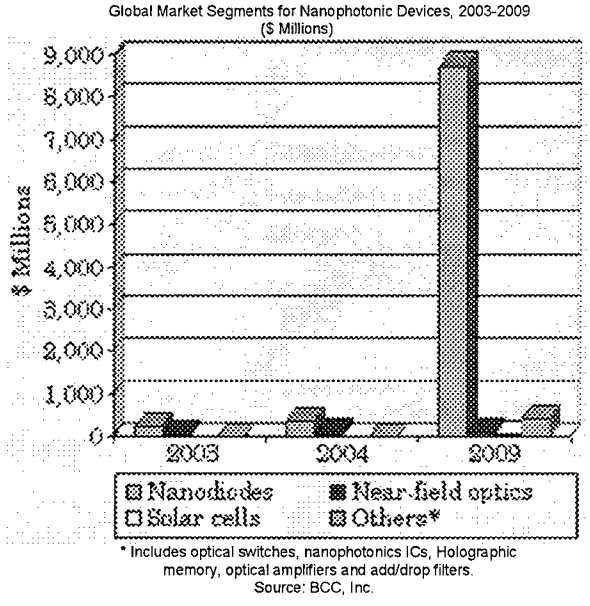

6.3 Market, Customer, and Competition

6.3.1 Market

We envision two major market areas for the low cost fabrication procedure for nano-structure based devices using chemical lithography, microscopy and nanolithography. The market size of these technologies is shown in Fig 45

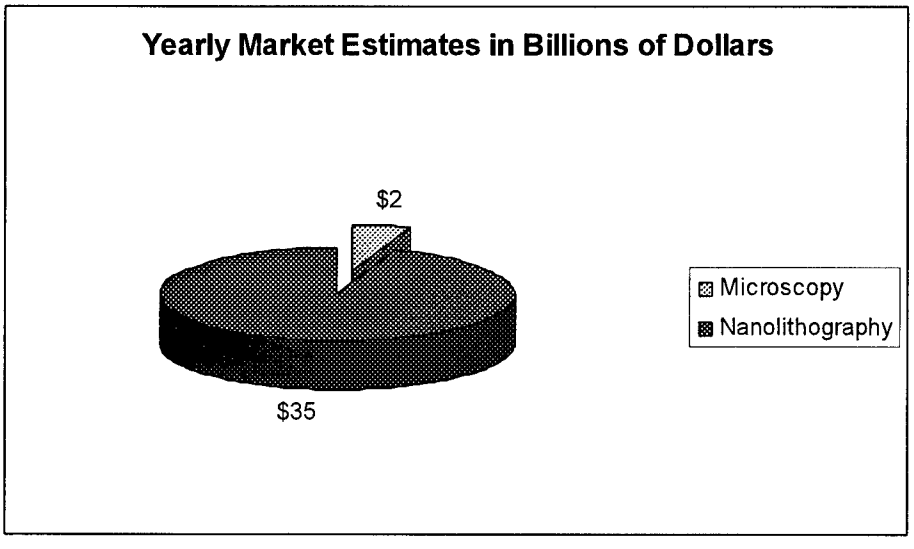

Figure 45. Worldwide Market Estimates for nanolithography, and Microscopy.

Microscopy plays a key role in enormous industries such as biomedicine and semiconductor manufacturing. A recent study released by Trimark publications (New York, NY) estimated the total microscopy market in 2000 at $2 billion (OE magazine, Nov. 2003).

Despite some overhype in the last few years, investment in nano technologies and applications continues to grow. For example, through its National Nanotechnology Initiative, the U.S. National Science Foundation (NSF) has spent more than $600 million to support R&D in this field since 1997. In addition, the NSF's Nanomanufacturing Program will spend $22 million this year to support fundamental research into the adaptation of technologies such as laser plasma vaporization, laser-guided particle transport, and laser tweezers for practical applications at the nanoscale. Such commitment appears to be paying off. According to a report published in July 2003 by The Freedonia Group (Cleveland, OH), an industrial market research firm, after a decade-long buildup, nanotechnology is beginning to see its first commercial successes. The Freedonia Group expects the U.S. market for nanomaterials (which totaled only $125 million in 2000) to surpass $1 billion in 2007 and reach $35 billion by 2020, with early growth coming from niche applications in manufacturing. These applications include wafer-polishing abrasives and high-density data-storage media for electronics; improved diagnostic aids for the medical community; The Freedonia Group believes the best opportunities are in health care and electronics, which together should account for nearly two-thirds of the market by 2020.(*Laser Focus World* September, 2003)

Nanotechnology is currently getting a lot of attention (and funding). In a market place with some shining stars, the promise to make things operate faster, more accurately, at a lower cost and in a smaller package makes nanotechnology the darling of many areas including homeland security.

Government attention to the true potential of nanotechnology started in 1993 and has been growing in interest and funding ever since. The National Science Foundation (NSF) estimates that global governmental spending on nano R&D was about $2.2 billion for year 2002. The NSF also predicts that the global market for nanotechnology-based applications such as our probe will surpass $1 trillion in little over a decade. The National Nanotechnology Investment (NNI) initiative FY2004 budget request allocates directly about $2 million for the Department of Home Land Security for nanotechnology research.

According to the SmallTimes e-sine, a nanotechnology advocacy group, this year along, venture capitalists and corporations are expected to invest 10 billion in American nanotechnology efforts.

A report by In-Stat/MDR, quoted by SmallTimes, predicts a $4 bullion market for biological and chemical based nano photonic based devices by 2007.

6.3.2 Customers

EM Photonics have identified near term and far term customers. Our near term customers will be manufacturers of chip scale optical signal and image processing units. Our far term customers will include physical and biological sciences and other micro-optic and Nano-MEMs technologies for chemical biosensors.

With this in mind, we have assembled a distinguished advisory board to guide us through the Phase II development effort. With feedback from our "customer base" during this stage of development we will be focused on addressing important requirements and specifications now, not during our Phase III commercialization. The advisory board will meet two to three times

during the project as a group and members will be available on an individual basis for feedback and suggestions.

6.3.3 Competition

We believe that this project provides a unique opportunity for EM Photonics, Inc. to utilize its micro and nano optical system expertise in developing fabrication procedures and technologies to fabricate ultra high resolution ADC and MSR systems Consultants and collaborators from the electronics field enhance the background and experience of EMP employees. However, we are not naïve and acknowledge that there are potential competitors that exist and may decide to move into this field. In particular, Molecular Imprints is a company that already markets lithography systems and technology for manufacturing applications in the areas of: nano devices, micro structures, advanced packaging, bio devices, optical components and semiconductor devices. Users of this technology have found them to be to be sensitive to alignment and orientation errors. Our technology and systems will be smaller and less invasive. Further, it can be engineered to serve both high and low volume production. There are several companies either manufacturing nanophotonic devices (Evident technologies, Nanonex) or providing fabrication services (Konarka, NanoHorizons) that currently are targeting the nano technology industry. These are large markets that our technology may also find application. However, we believe that our team and our interest in building the product around the needs of the semiconductor community will differentiate us from our competition.

6.3.4 Intellectual Property Protection

At our current stage, EMP recognizes that its major asset is its intellectual property. Therefore, a patent disclosure process was instituted at the company's inception. In this time, 6 disclosures on various products have been filed. A disclosure has been submitted regarding aspects of this work. In addition, all employees are required to sign non-disclosure and non-compete agreements. Contractors are also required to sign an agreement before any work takes place.

For the chemical nanophotonic devices program, the strength of our team, its diversity, the emphasis on near and far term applications, and the contributions of representative customers during the Phase II development will result in a superior product. We believe that this will provide at least a temporary barrier to competition.

6.3.5 Finance Plan

We believe that significant product development can be achieved with the Phase II funding. In fact, as part of our Phase II plan we intend to perform extensive testing which is relevant to our customer's interest. Based on this work, we envision that a product will be available for use in these settings immediately after Phase II. Concurrent with the nano-probe development, we will dedicate considerable effort to physical and biological sciences and other micro-optic and Nano-MEMs technologies for chemical biosensors.

The overall EM Photonics business plan calls for a major investment (~$5 million) after our initial development stage. This investment will give EM Photonics greater fabrication capability and allow us to serve a variety of micro and nano photonics markets. We have met with potential investors and at this point feel it is still early. Should a product opportunity arrive before we are ready for the large-scale investment, we will identify an investor that has specific interest in that product line.

6.3.6 Production and Marketing Plan

6.3.6.1 Production Plan

In collaboration with University of Delaware, we will test and push the fundamental resolution limits of photonic crystal devices. This will require the fabrication of high resolution templates, exploring alternative methods of application of catalyzing acid, investigating the effect of environmental conditions on the fidelity of obtained patterns, developing methodology for acid transfer, exploring various chemistries of the process, controlling the diffusion of the acid throughout the volume of the resist. All these aspects of process development are described in more detail in the project summary section. We will further work closely with our to facilitate the integration of our technology to their next generation product line.

6.3.6.2 Marketing Plan

As a small business that is developing new technology, we currently utilize the following marketing strategy.

1. Present papers, tutorials, and/or attend key scientific conferences where representatives from funding agencies, early adopters and potential collaborators are in attendance.
2. When possible, maintain a booth at the exhibitor section of the key conferences.
3. Collect contact information from responders to presentations and booths.
4. Maintain a customer database that can be searched by keywords.
5. Create and send product literature to potential customers.
6. Maintain an up to date website with project and product information

In 2003, we exhibited at the Conference on Lasers and Electro-Optics (CLEO) and the Optical Society of America Meeting on Integrated Photonics Research. See Figure 3. In addition, EMP employees were in attendance at SPIE, Photonics West and SPIE, AeroSense to attend presentations relevant to our product development.

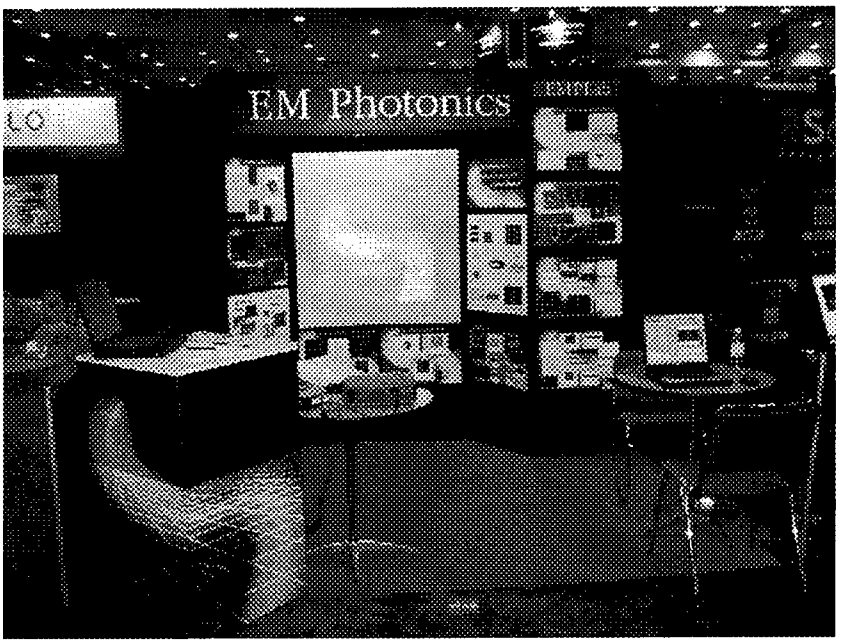

Figure 46. EM Photonics, Inc. Booth at CLEO, Baltimore, 2003.

In marketing chemically lithographic based devices; we have identified the following conferences for the introduction of the technology to potential customers

1. The international society for optical engineering (SPIE), Near Field Optics: Physics, Devices, and Information Processing
2. National institute of standards and technology (NIST) Near-field Scanning Optical Microscopy (NSOM)
3. American Physical Society, APS
4. Conference of lasers and electro optics/international quantum electronics conference (CLEO/IQEC)
5. IEEE sensors conference
6. Optical MEMS conference
7. Optical Fiber Communication conference OFC

The SPIE meeting will focus on near-field optics and nanolithography and how it has evolved as a very effective bridge between the ubiquitous and ever expanding worlds of lithographically fabricated optical devices. The conference will be focused on all aspects of lithography and its related applications that are based on techniques. However our novel chemical lithography based fabrication procedures, which overcomes the production limitations and percentage yield of current systems will set the standards for next generation lithographically prescribed optoelectronic devices. NIST, APS, CLEO NFO, and ODS will mainly focus in the applications of our fabrication processes to various areas in science and technology, while OFC will mainly focus in commercializing our technology by combining a high-powered, commerce-driven exposition with leading-edge, peer reviewed educational programming. This unique combination makes the conference among the field's most important events. Professionals from all disciplines within optical communications attend this conference to: see/evaluate new products and developments attend educational sessions; keep up to date on industry trends and issues.

These activities will be necessary, as researchers in an experimental environment will use our product. Feedback from attendees should help us focus on performance features that are most relevant and have the best opportunity. By offering the optical force sensor at conferences, EMP will likely identify additional collaborations and product development opportunities in the medical device field.

As our product evolves and awareness increases, eventually we will be able to sell standard components and accessories. At this point, we can sell from product and option lists from our website or a catalog.

6.3.6.3 Revenue Stream

We envision that an early revenue stream may exist in the form of consulting and collaborative research efforts that investigate the application of this nano-probe Engineering, Physics, chemistry and biology fields that we have mentioned. As interest and acceptance of the technology increases, we believe that revenues will be generated by the sale of nano probes and the various applications and equipments they go into. At the moment, we estimate that lithography equipment costs will run from $100,000 to $500,000 depending on the level of complexity (speed, resolution, yield, etc.) of the measurement. If we were to consider the nano-imprint system a stand-alone module. Eventually, we intend to sell a range of systems from an inexpensive form, (less than $100,000/system) to ultra-high resolution systems (~$250,000-$400,000/system) for high volume applications.

EM Photonics is excited about marketing this product. We believe that we can reach commercial viability upon completion of the Phase II program. It is a realistic first product for our company to offer within the semiconductor market that will lead to further commercial opportunities. Affordable ultra high resolution nano-imprint systems will be an enabling technology for the development of many nano-features size devices and systems and offers the potential for significant contributions to many fields of biomedical and chemical engineering.